monkeys expressing a mutant human huntingtin gene. In that report, although the transgene was inserted into the genome of founder infants and its expression was detected in post-mortem animals, the germline transmission of the transgene has not yet been confirmed[7]. Thus, at this point, it is not certain how reproducible the effects of various therapeutic interventions would be using a large number of animals.

The technique by which we achieved transgene expression in several tissues, along with germline transmission, may provide the means to obtain genetically modified non-human primate models for translational research, investigations of regenerative medicine and gene therapy, and clarification of the scientific gaps among transgenic mice, human disease models, and real human diseases.

METHODS SUMMARY

All animal experiments were approved by the institutional animal care and use committee, and were performed in accordance with Central Institution for Experimental Animal (CIEA) guidelines.

To obtain oocytes, recombinant human follicle stimulating hormone (r-hFSH; 50 international units (IU); Fertinome, Serono) was administered daily by intramuscular injection for 11 days. Human chorionic gonadotropin (hCG; 75 IU; Gonatropin, Teikoku-zouki) was administered by intramuscular injection at 17:30 on day 12. On day 13, the animals were anaesthetized and follicular aspiration was performed surgically. Oocytes were incubated for 24 h at 38 °C, 5% CO_2 in air, for *in vitro* maturation. After incubation, only matured oocytes (metaphase II) were collected and used for IVF.

Ejaculated semen was collected in TYH medium (Mitsubishi Kagaku Iatron), using a Ferti Care personal vibrator. Hyaluronidase-treated oocytes were placed in 70-μl drops of TYH, and an aliquot of sperm (4×10^5) was added to each oocyte incubation drop. After 26–30 h of insemination, the fertilized oocytes were placed into ISM1 (Medicult) medium, and lentiviral vector injection was performed in 0.25 M sucrose.

Natural embryo collection was performed as previously described[21]. Embryos at the pronuclear-to-morula stage were placed in 0.25 M sucrose supplemented PBI medium (Mitsubishi Chemical Medience Corporation) and injected with lentiviral vector. Blastocysts were not treated with sucrose. Lentiviral vector injection was performed using an Eppendorf FemtoJet express and a Narishige micromanipulator. The embryos were cultured until GFP expression was confirmed.

The ovulation cycles of donor and recipient animals were synchronized, and EGFP-expressing embryos were transferred as previously described[22,23]. After embryo transfer, the recipients were tested for pregnancy by plasma progesterone once a week. The resulting infants were analysed for transgene integration, transcription and expression, by real-time PCR, Southern blot analysis, RT–PCR, immunohistochemical analysis, FACS and FISH.

Full Methods and any associated references are available in the online version of the paper at www.nature.com/nature.

Received 27 September 2008; accepted 30 April 2009.

1. Mansfield, K. Marmoset models commonly used in biomedical research. *Comp. Med.* **53**, 383–392 (2003).
2. Chan, A. W., Homan, E. J., Ballou, L. U., Burns, J. C. & Bremel, R. D. Transgenic cattle produced by reverse-transcribed gene transfer in oocytes. *Proc. Natl Acad. Sci. USA* **95**, 14028–14033 (1998).
3. Hofmann, A. *et al.* Efficient transgenesis in farm animals by lentiviral vectors. *EMBO Rep.* **4**, 1054–1060 (2003).
4. Hofmann, A. *et al.* Generation of transgenic cattle by lentiviral gene transfer into oocytes. *Biol. Reprod.* **71**, 405–409 (2004).
5. Chan, A. W., Chong, K. Y., Martinovich, C., Simerly, C. & Schatten, G. Transgenic monkeys produced by retroviral gene transfer into mature oocytes. *Science* **291**, 309–312 (2001).
6. Wolfgang, M. J. *et al.* Rhesus monkey placental transgene expression after lentiviral gene transfer into preimplantation embryos. *Proc. Natl Acad. Sci. USA* **98**, 10728–10732 (2001).
7. Yang, S. H. *et al.* Towards a transgenic model of Huntington's disease in a non-human primate. *Nature* **453**, 921–924 (2008).
8. Rogers, C. S. *et al.* Disruption of the *CFTR* gene produces a model of cystic fibrosis in newborn pigs. *Science* **321**, 1837–1841 (2008).
9. Rogers, C. S. *et al.* Production of *CFTR*-null and *CFTR-ΔF508* heterozygous pigs by adeno-associated virus-mediated gene targeting and somatic cell nuclear transfer. *J. Clin. Invest.* **118**, 1571–1577 (2008).
10. Miyoshi, H., Blomer, U., Takahashi, M., Gage, F. H. & Verma, I. M. Development of a self-inactivating lentivirus vector. *J. Virol.* **72**, 8150–8157 (1998).
11. Ross, C. N., French, J. A. & Orti, G. Germ-line chimerism and paternal care in marmosets (*Callithrix kuhlii*). *Proc. Natl Acad. Sci. USA* **104**, 6278–6282 (2007).
12. Takahashi, K. *et al.* Induction of pluripotent stem cells from adult human fibroblasts by defined factors. *Cell* **131**, 861–872 (2007).
13. Yu, J. *et al.* Induced pluripotent stem cell lines derived from human somatic cells. *Science* **318**, 1917–1920 (2007).
14. Byrne, J. A. *et al.* Producing primate embryonic stem cells by somatic cell nuclear transfer. *Nature* **450**, 497–502 (2007).
15. Nakagawa, M. *et al.* Generation of induced pluripotent stem cells without Myc from mouse and human fibroblasts. *Nature Biotechnol.* **26**, 101–106 (2008).
16. Iwanami, A. *et al.* Transplantation of human neural stem cells for spinal cord injury in primates. *J. Neurosci. Res.* **80**, 182–190 (2005).
17. Thomson, J. A. *et al.* Embryonic stem cell lines derived from human blastocysts. *Science* **282**, 1145–1147 (1998).
18. Iwanami, A. *et al.* Establishment of graded spinal cord injury model in a nonhuman primate: the common marmoset. *J. Neurosci. Res.* **80**, 172–181 (2005).
19. Eslamboli, A. Marmoset monkey models of Parkinson's disease: which model, when and why? *Brain Res. Bull.* **68**, 140–149 (2005).
20. Ando, K. *et al.* Neurobehavioral protection by single dose l-deprenyl against MPTP-induced parkinsonism in common marmosets. *Psychopharmacology (Berl.)* **195**, 509–516 (2008).
21. Sasaki, E. *et al.* Establishment of novel embryonic stem cell lines derived from the common marmoset (*Callithrix jacchus*). *Stem Cells* **23**, 1304–1313 (2005).
22. Lopata, A., Summers, P. M. & Hearn, J. P. Births following the transfer of cultured embryos obtained by *in vitro* and *in vivo* fertilization in the marmoset monkey (*Callithrix jacchus*). *Fertil. Steril.* **50**, 503–509 (1988).
23. Summers, P. M., Shephard, A. M., Taylor, C. T. & Hearn, J. P. The effects of cryopreservation and transfer on embryonic development in the common marmoset monkey, *Callithrix jacchus*. *J. Reprod. Fertil.* **79**, 241–250 (1987).

Supplementary Information is linked to the online version of the paper at www.nature.com/nature.

Acknowledgements We thank F. Toyoda, S. Ohba, T. Inoue, Y. Sawada and M. Yokoyama for technical assistance with the animal experiments and care. E.S. is an associate professor of the Global COE program for human metabolomic systems biology assigned to Keio University. This study was also supported by the Global COE program for Education and Research Centre for Stem Cell Medicine from the Ministry of Education, Culture, Sports, Science and Technology (MEXT), the Japanese Government to Keio University. This study was also supported by funds from Solution-Oriented Research for Science and Technology (SORST) of the Japan Science and Technology Agency and grants from MEXT to H.O. and from Special Coordination Funds for Promoting Science and Technology of MEXT to S.H.

Author Contributions E.S. designed the experiments, conducted the project, and wrote the paper. A.S., Y.S., T.E., I.T. and R.H. assisted in embryological technique development. K.H., R.O. and M.K. developed surgical techniques for embryo collection and transfer. H.S., C.K. and C.Y. performed or assisted with the real-time PCR and parentage evaluation test. S.S. and T.M. assisted with the Southern blot analysis and tissue collection. M.I. raised the anti-marmoset CD45 antibody. R.I. performed the FACS analysis, and K.K. performed the immunohistochemical analysis. H.M. provided the lentiviral vectors. Y.T., H.O., S.H., N.T. and T.N. designed the project, and H.O., S.H. and N.T. also participated in writing the paper. The whole project was supervised by E.S. and H.O.

Author Information Reprints and permissions information is available at www.nature.com/reprints. Correspondence and requests for materials should be addressed to E.S. (esasaki@ciea.or.jp) or H.O. (hidokano@sc.itc.keio.ac.jp).

METHODS

Animals. Adult common marmosets more than 2 years old were obtained from a marmoset breeding colony for experimental animals. Female marmosets with normal ovarian cycles were paired with intact males for natural embryo collection. Recipient females were paired with vasectomised males or intact females. This study was approved by the Institutional Animal Care and Use Committee of CIEA, and was performed in accordance with CIEA guidelines.

***In vitro* fertilization.** Semen was collected as previously described for common marmosets[24]. Ejaculated semen was collected in TYH medium (Mitsubishi Kagaku Iatron) and washed twice with TYH. The semen was placed in a CO_2 incubator for 10 min in a test tube inclined at a 30° angle to allow the sperm to swim up. Hyaluronidase-treated metaphase-II-arrested oocytes were inseminated with a final concentration of 5×10^6 sperm ml^{-1} for 26–30 h. Fertilized embryos were cultured in ISM medium (Medicult, Nosan Corp.).

Embryo collection and transfer. Embryo collection and transfer were performed as previously described[25]. After embryo transfer, the recipients were monitored for pregnancy by measuring their plasma progesterone once a week until the pregnancies could be monitored by transabdominal palpation of the uterus.

Lentiviral vector preparation and transduction. The lentiviral vectors were produced as previously described[26]. The medium containing viral particles was spun at 4 °C, 50,000*g* for 4 h, and the viral pellet was then resuspended in ISM2 medium, in 1/1,000 of the volume of the original lentiviral vector supernatant. To measure the lentivirus titre, serially diluted (10^{-2} to 10^{-8}) lentiviral vector was used to infect 10^5 293T cells. The number of EGFP-positive cells was counted by FACS to quantify the titre.

Pronuclear-to-morula stage embryos were placed in 0.25 M sucrose supplemented PB1 medium (Mitsubishi Chemical Medience Corporation), and the virus was injected into the perivitelline space. For blastocyst embryos, the viral vector was injected into the blastocoel. All viral injections were performed using an Eppendorf FemtoJet Express and a Narishige micromanipulator.

Southern blot analysis. Five micrograms of genomic DNA was digested with BamHI for animals that had been injected with CAG-EGFP, and with EcoRI for those that had been injected with CMV-EGFP. The digested genomic DNA was separated on a 0.8% agarose gel and transferred to a Hybond-N+ nylon membrane (GE Healthcare Biosciences). Southern blot analysis was performed using the DIG system (Roche Diagnostics K.K.), according to the manufacturer's protocol. CMV-EGFP was digested with EcoRI and then labelled with DIG using the PCR DIG probe synthesis kit, according to the manufacturer's instructions (Roche Diagnostics K.K.).

RT–PCR. To detect EGFP gene expression, EGFP5-5 (5′-GCACAAGCTGGAGTACAACTACAACAGC-3′) and EGFP3-1 (5′-TCACGAACTCCAGCAGGACCAT-3′) primers were used. To detect β-actin expression, β-actin 001 (5′-TCCTGACCCTGAAGTACCCC-3′) and β-actin 002 (5′-GTGGTGGTGAAGCTGTAGCC-3′) primers were used. PCR was performed for 35 cycles of denaturation at 94 °C for 30 s, annealing for 30 s at 58 °C for EGFP primers or 62 °C for β-actin primers, and elongation at 72 °C for 30 s.

To detect EGFP gene expression in germ cells and neonatal tissues, PCR was performed using the EGFP5-4 (5′-CAAGGACGACGGCAACTACAAGACC-3′) and EGFP3-3es (5′-GCTCGTCCATGCCGAGAGTGA-3′) primers. Then, 1 μl of the PCR products was re-amplified with the EGFP5-6 (5′-TCGAGCTGAAGGGCATCGAC-3′) and EGFP3-1 (5′-TCACGAACTCCAGCAGGACCAT-3′) primers. To detect β-actin expression, the PCR primers β-actin 003 (5′-TGGACTTCGAGCAGGAGAT-3′) and β-actin 006R (5′-CCTGCTTGCTGATCCACATG-3′) were used. Then, 0.5 μl of the PCR products was re-amplified with the 004 (5′-TCCCTGGAGAAGAGCTATG-3′) and 005R (5′-GAGCCACCAATCCACACTGA-3′) primers. PCR was performed for 30 cycles of denaturation at 98 °C for 10 s, annealing at 60 °C for 10 s, and elongation at 72 °C for 30 s.

Immunohistochemical analysis. Tissues were embedded in OCT compound, frozen in liquid nitrogen, and sliced into 5-μm sections, which were fixed in 4% paraformaldehyde for 30 min at 4 °C. Endogenous peroxidase activity was quenched using 0.03% hydrogen peroxidase for 30 min at room temperature. The slides were blocked with 10% goat serum (Nichirei) for 10 min at room temperature and then reacted with the rabbit anti-GFP polyclonal antibody (A.v. peptide antibody, BD Bioscience) overnight at 4 °C. The slides were incubated with the biotinylated secondary antibody Simple Stain Mouse MAX PO (Nichirei) for 30 min at room temperature. The bound antibodies were detected with DAB (3,3-diaminobenzidine tetrahydrochloride) horseradish peroxidase complex. The samples were then stained with H&E and examined by microscopy.

FACS analysis. Whole blood cells were washed with PBS and suspended in 0.13 M NH_4Cl. The pellet was incubated with the mouse IgG1 anti-marmoset CD45, 6C9 antibody for 30 min on ice[27], then mixed with an allophycocyanin (APC)-labelled anti-mouse IgG antibody, and incubated for 30 min on ice. The sample was washed with PBS and resuspended in 200 μl of propidium iodide solution. FACScant analysis was then performed.

Fluorescent *in situ* hybridization. Peripheral blood samples were cultured in RPMI 1640 containing phytohaemagglutinin, concanavalin A, lipopolysaccharide, and 2-mercaptoethanol for 2–3 days. After 2–3 h of incubation with BrdU (final concentration 30 μg ml^{-1}), colcemid (final concentration 0.02 μg ml^{-1}) was added to the medium, and the samples were incubated for another 2 h. After lymphocyte fixation, the cells were spread on slides and air-dried overnight, then stained with Hoechst 33258 and treated with ultraviolet light. CAG-EGFP was labelled with digoxigenin-11-dUTP as a probe, and hybridized at 37 °C overnight. After stringent washes, the bound label was detected using anti-Dig-Cy3. For karyotyping, Leica CW4000 FISH and Leica CW4000 Karyo were used.

24. Kuederling, I., Schneiders, A., Sonksen, J., Nayudu, P. L. & Hodges, J. K. Non-invasive collection of ejaculates from the common marmoset (*Callithrix jacchus*) using penile vibrostimulation. *Am. J. Primatol.* 52, 149–154 (2000).
25. Summers, P. M., Shephard, A. M., Taylor, C. T. & Hearn, J. P. The effects of cryopreservation and transfer on embryonic development in the common marmoset monkey, *Callithrix jacchus*. *J. Reprod. Fertil.* 79, 241–250 (1987).
26. Bai, Y. *et al.* Effective transduction and stable transgene expression in human blood cells by a third-generation lentiviral vector. *Gene Ther.* 10, 1446–1457 (2003).
27. Ito, R. *et al.* Novel monoclonal antibodies recognizing different subsets of lymphocytes from the common marmoset (*Callithrix jacchus*). *Immunol. Lett.* 121, 116–122 (2008).

Artificial Organs

Artificial Organs
33(2):169–176, Wiley Periodicals, Inc.

Effects of Liposome-Encapsulated Hemoglobin on Human Immune System: Evaluation in Immunodeficient Mice Reconstituted With Human Cord Blood Stem Cells

*Akira T. Kawaguchi, *Yoshie Kametani, *Shunichi Kato, *Hiroyuki Furuya, †Kenichi Tamaoki, and *Sonoko Habu

**Tokai University School of Medicine; and †Central Institute for Experimental Animals Kanagawa, Japan*

Abstract: As preclinical evaluation in animals does not necessarily portray human responses, liposome-encapsulated hemoglobin (LEH), an artificial oxygen carrier, was tested in immunodeficient mice reconstituted with human hematopoietic stem cells (cord blood-transfused NOD/SCID/IL-2R$_{\gamma null}$ [CB-NOG] mice). Changes in immunocompetent T-cell and B-cell composition in peripheral blood, spleen, and bone marrow were examined 2 and 7 days after 10 mL/kg of intravenous administration of LEH, empty liposome (EL), or saline using immunohistochemical and flow cytometrical techniques in wild-type mice and CB-NOG mice. Responses to intraperitoneal administration of toxic shock syndrome toxin-1 (TSST-1) under the absence or presence of LEH (10 mL/kg) were also determined 4 h and 3 days later in terms of lymphocyte composition and IL-2 plasma level in wild-type as well as CB-NOG mice. When liposome (LEH or EL) was administered to wild-type or CB-NOG mice, the composition of B-cells and T-cells in the spleen or peripheral blood failed to show any consistent or significant changes. The responses to a bacterial antigen (TSST-1) measured by IL-2 production were comparable regardless of the presence or absence of LEH in wild-type as well as in CB-NOG mice. Cellularity, distribution, and maturation of these human cells in peripheral blood, spleen, and bone marrow were comparable among the groups. The results suggest that simple LEH administration may not change immune cellularity, and LEH presence may not largely affect the early T-cell response to bacterial enterotoxins in murine as well as in reconstituted human immune systems.
Key Words: Artificial oxygen carrier—Liposome-encapsulated hemoglobin—Human immune system—Immune response—Toxic shock syndrome toxin-1—NOG mice—Cord blood—Stem cells.

Artificial oxygen carriers have been developed as a substitute of red blood cells (RBCs). As blood circulation provides the whole body with metabolism and defense, its replacement in quantity may naturally influence hemodynamics and immune status. While cell-free hemoglobins have been associated with vasoactive properties (1,2), encapsulation and pegylation (3,4) in the form of liposome-encapsulated hemoglobin (LEH) appeared to have avoided such adverse events in the rat (5), as well as in nonhuman primate (6). Nonetheless, its effect on the immune system has not been fully explored (7). As preclinical safety evaluation of a new regimen in animals does not always predict human responses, as in the case of TGN1412, an anti-CD28 monoclonal antibody (8), which caused serious diseases in humans although it was not toxic in the preclinical testing in animals (9), animals with a human immune system are desirable to better serve as a preclinical test for safety evaluation, offering a better scope of human responses and possibly reducing risks in humans undergoing phase 1 studies. We have developed a human immune system reconstituted in the mouse environment (10,11) by transplanting human hematopoietic stem cells from umbilical cord blood into immunodeficient NOD-SCID-IL-2RγKO mice (12). This cord blood-transfused NOD/SCID/IL-2R$_{\gamma null}$ (CB-NOG) mouse has been proven to be partly immunocompetent; human hematopoietic stem cells develop

doi:10.1111/j.1525-1594.2008.00703.x

Received March 2008; revised September 2008.
Address correspondence and reprint requests to Dr. Akira T. Kawaguchi, Tokai University School of Medicine, Bohseidai, Isehara, Kanagawa 259-1193, Japan. E-mail akira@is.icc.u-tokai.ac.jp
Presented in part at the 2007 Joint Congress of Japanese Society for Artificial Organs and the International Federation for Artificial Organs held on October 28–31, 2007 in Osaka, Japan.

lymphocytes, but do not efficiently produce myeloid cells (12). The T-cell–B-cell interaction is not sufficiently performed and antigen-specific IgG is not detected after immunization of conventional antigens in CB-NOG mice (10,13). Therefore, we focused on changes in T-cell and B-cell composition and the reactivity of T-cells to a superantigen in the presence or absence of LEH in CB-NOG mice, as well as in wild-type BALB/c mice as a murine control, first with simple intravenous administration (Protocol I), and then affecting the immunological response to a superantigen in the presence or absence of LEH (Protocol II).

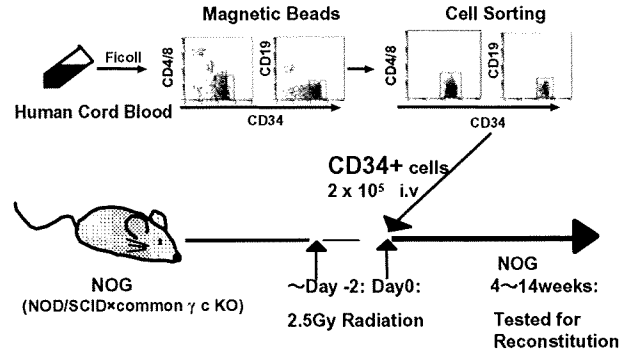

FIG. 1. CB-NOG mice. Preparation of CB-NOG mice. Details are described in the text.

MATERIALS AND METHODS

Liposome-encapsulated hemoglobin (LEH)

Relevant characteristics of LEH (cord name: TRM-645, Terumo, Co., Ltd., Tokyo, Japan) have been reported (4–7). Briefly, this liposome capsule, measuring 230 nm in mean diameter, contains human hemoglobin purified from donated blood outdated for transfusion. The liposome capsule was coated with polyethylene glycol to reduce aggregation and recognition by the reticuloendothelial cell system, as well as to prolong the circulatory half-life to 30–50 h in the primate (6). In this preparation, inositol hexaphosphate was used to control O_2 affinity to P_{50} = 40–50 mm Hg in LEH (TRM-645) (4,5), lower than that of rodent RBC (P_{50} = 30 mm Hg). LEH was suspended in saline at a hemoglobin concentration of 6 g/dL or 25% of volume, which has a reduced viscosity (2 cp) compared with blood (5 cp) and a specific gravity close to that of plasma. Empty liposome (EL) was prepared exactly as LEH except for the inclusion of saline instead of human hemoglobin to serve as a nonoxygen carrying control solution.

Animals

NOD/Shi-scid, common γc-null (NOD/SCID/γc-null; NOG, Fig. 1) mice were provided by the Central Institute for Experimental Animals (Kawasaki, Japan). BALB/c mice were purchased from CREA Japan Inc. (Kawasaki, Japan) to serve as wild-type murine control. All mice were kept under specific pathogen-free conditions in the animal facility of the Tokai University School of Medicine (Isehara, Japan).

CB-NOG mouse

Human umbilical cord blood was obtained from full-term healthy newborns immediately after vaginal delivery. Informed consent was obtained according to the institutional guidelines, and this work was approved by the Tokai University Human Research Committee. Mononuclear cells (MNCs) were separated by Ficoll-Paque gradient centrifugation (Fig. 1). CD34+ cells were purified from MNCs using the two-step magnetic cell sorting system (Miltenyi Biotec, Gladbach, Germany). Purity was more than 98%. Nine-week-old NOG mice were sublethally irradiated with 2.5 Gy prior to the transplantation, and CD34+ cells were transplanted intravenously. Eight weeks after the transplantation, peripheral blood was collected via orbit under inhalation anesthesia. MNCs were prepared and reconstitution efficiencies were calculated by human CD45 expression analyzed by fluorescence-activated cell sorter (FACS) analysis. Final reconstitution efficiency was calculated by the human CD45+ cell percentage of CB-NOG bone marrow. The mean CD45+ cells were (percentages ± SD): phosphate buffered saline (PBS) group, 55.9 ± 19.9%, EL group, 60.5 ± 29.7%, and LEH group, 55.2 ± 19.2%. The mice were used at 15–22 weeks posttransplantation, as both human T-cells and B-cells were detectable in this period.

Monoclonal antibodies and flow cytometry

Each antibody was added to the cells (10^6) and incubated in the dark for 15 min at 4°C. Cells were washed and analyzed by FACS Caliber (Becton Dickinson, Franklin Lakes, NJ, USA). For each analysis, living gated white blood cells or lymphocytes were further gated on human CD45+ cells. The populations of naïve/activated/memory T-cells were also evaluated by the expression of CD25, CD44, CD62L, or CD69 in an overall or CD4-gated window for T-cells. The following mouse antihuman monoclonal antibodies were used: PerCP-conjugated CD45, TCR, CD1a, fluorescein isothiocyanate-conjugated CD4, IgM, phycoerythrin-conjugated CD4, CD8, IgD, and APC-conjugated CD19.

TSST-1 administration and enzyme-linked immunosorbent assay (ELISA)

Fifteen to twenty-two weeks after the transplantation, mice were administered intraperitoneally with toxic shock syndrome toxin-1 (TSST-1, 25 μg/alum/head, Toxin Tec, Sarasota, FL, USA). ELISA for human IL-2 production was performed according to the manufacturer's instruction (and as described previously [11]) before, 4 h after, and 3 days after TSST-1 administration using the sera of the mice. Then, at 3 days, the mice were sacrificed, and spleen cells, bone marrow, and peripheral blood were collected for cell composition analyses.

Histochemistry

Spleen pieces were fixed in 20% formalin solution, embedded in paraffin, sectioned (4 μm), and stained with hematoxylin and eosin. For the immunohistochemical study, the spleen was frozen, freshly embedded in optimal cutting temperature compound (Sakura Tissue-Tek Oct Compound, International Medical Equipment Inc., San Marcos, CA, USA), cryostat sectioned (6 μm), and serially stained with saturating amounts of the following monoclonal antibodies (100-fold dilution): CD20 for human B-cells and CD3 for human T-cells for CB-NOG mice, and B220 for murine B-cells or Thy-1.2 for murine T-cells for BALB/c mice.

Protocol I

In order to study the effect of simple intravenous infusion, or top-load of LEH (Fig. 2A), changes in immunocompetent cells in peripheral blood and spleen were examined 2 and 7 days after 10 mL/kg of intravenous infusion of LEH, EL, or PBS using flow-cytometrical technique and immunohistochemical staining in wild-type mice (each group, $n = 4$) as well as in CB-NOG mice (each group, $n = 4$). Because of the technical complexity and availability of CB-NOG mice, each experiment included only three animals, each receiving PBS, EL, or LEH, which were housed together in the same cage before sacrifice at 2 or 7 days depending on the protocol. The experiments were repeated four times before sacrifice at 2 days (each group, $n = 4$), and an additional four times before sacrifice at 7 days (each group, $n = 4$), as the CB-NOG mice became available (Fig. 2A).

Protocol II

In order to evaluate the effect on the active immunological response to a third-party antigen in the presence of LEH, changes in immunocompetent cells in peripheral blood, spleen, and bone marrow were studied 3 days after TSST-1 administration with or without the presence of LEH in BALB/c mice as well as in CB-NOG mice (Fig. 3A). The plasma level of IL-2 was sequentially monitored before, at 4 h, and at 3 days after intraperitoneal administration of TSST-1 in each mouse immediately after infusion of 10 mL/kg of LEH (LEH+, $n = 4$) or 10 mL/kg of PBS (PBS+, $n = 4$) in wild-type as well as in CB-NOG mice. Because of technical complexity and availability of CB-NOG mice, each experiment included only four animals, each receiving PBS or LEH with or without TSST-1 administration, housed together in the same cage, and sacrificed 3 days later. The experiments were repeated four times using wild-type BALB/c mice ($n = 4$) and nine times using CB-NOG mice ($n = 9$).

Statistics

Data were presented as mean ± SD. The relative population of cells and IL-2 levels were averaged for each group of mice and compared among the groups by unpaired t-test. Time-bearing changes in single groups were tested by paired t-test or Kruskal–Wallis test for comparison among two or more groups. A P value less than 0.05 was considered statistically significant.

RESULTS

Protocol I: Simple administration, top-load

Changes in immunocompetent cell composition (Fig. 2B) by FACS analysis (%) in the spleen and peripheral blood for BALB/c mice and CB-NOG mice are shown before as a pretreatment reference, at 2 and 7 days after the intravenous administration of 10 mL/kg of PBS, EL, or TRM-645 (LEH). The component changes of these cells were not significantly different regardless of the solution infused in the BALB/c mice as well as in the CB-NOG mice. While variations in wild-type mice were small, there was a tendency toward an increased variation in CB-NOG mice. Moreover, there was no significant increase in activated T-cells in any mice or at any observation time point (data not shown).

Protocol II: Effects of LEH on responses to a third-party antigen, TSST-1

Changes in immunocompetent cell composition (Fig. 3B) by FACS analysis (%) in the spleen, peripheral circulating blood, and bone marrow in BALB/c mice as well as in CB-NOG mice are shown 3 days after with or without the intraperitoneal administration of TSST-1 in the absence or presence of the prior infusion of LEH. While the cell population and composition were similar

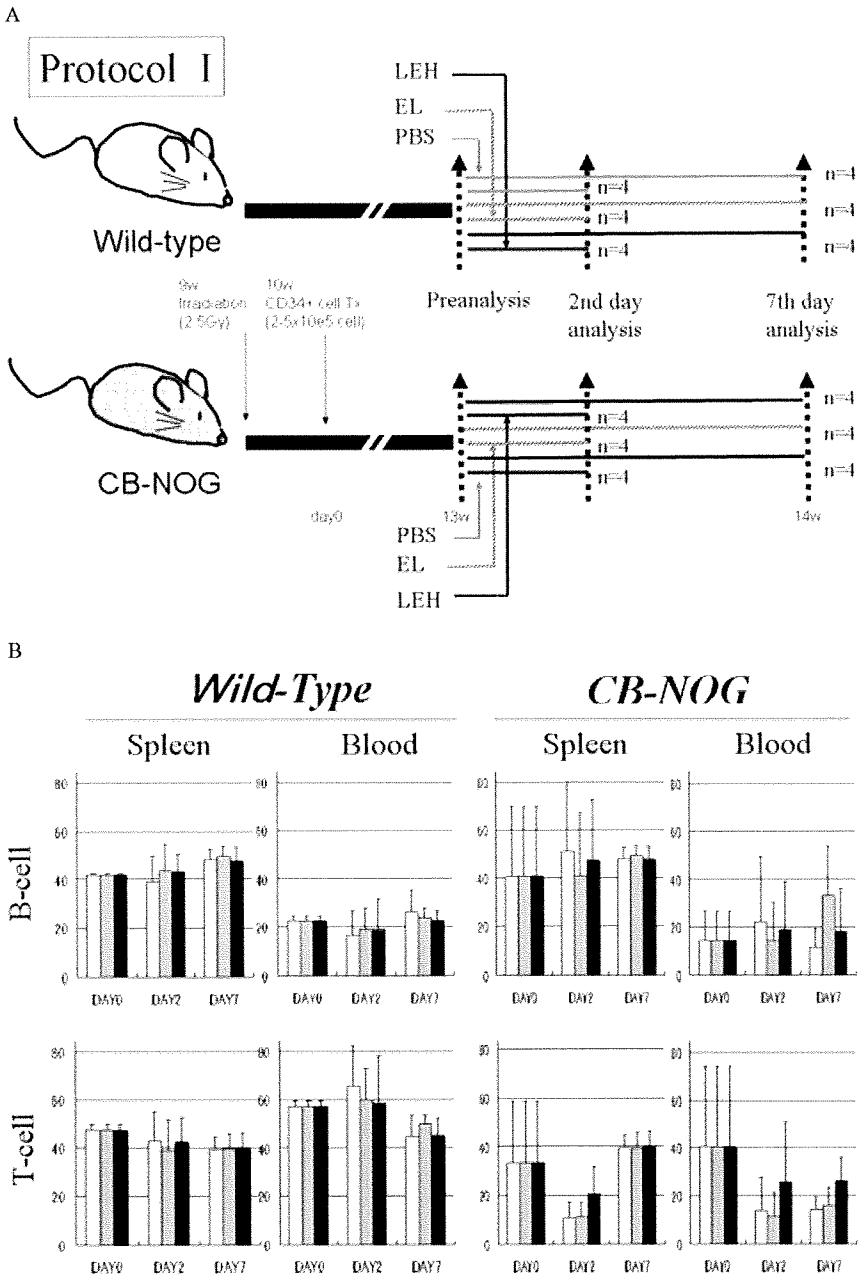

FIG. 2. Immunocompetent cell population changes after simple administration. (A) Protocol I: Effects of simple administration (top-load). (B) Changes in B-cell and T-cell population after administration of saline (PBS, open columns), empty liposome (EL, masked columns), and TRM-645 (LEH, closed columns) in BALB/c (Wild-type) and CB-NOG (CB-NOG) mice in the spleen (Spleen) as well as in peripheral blood (Blood).

between BALB/c and CB-NOG mice, significant changes in response to TSST-1 were observed only in the wild-type mice; B-cells in the peripheral blood and bone marrow were significantly suppressed in response to TSST-1 both in the saline-treated and LEH-treated wild-type mice. There was a significant increase in peripheral blood T-cells in response to TSST-1 in LEH-treated mice, but not in the saline-treated wild-type mice. This was the only discrepancy regarding the presence or absence of LEH in response to TSST-1 in wild-type mice, which was not observed in CB-NOG mice.

IL-2 production

Changes in the plasma level of IL-2 were sequentially (before, at 4 h, and at 3 days) monitored in the total of eight (2^3) groups of mice with or without intraperitoneal administration of TSST-1 in CB-NOG as well as in wild-type mice in the presence or absence of LEH (Fig. 3C). The plasma levels of IL-2 remained at baseline in any of the mice not receiving intraperitoneal TSST-1. Mice treated with TSST-1 showed increased plasma levels of IL-2 in a similar pattern and returned to baseline 3 days later regardless of the presence or absence of LEH, saline, or

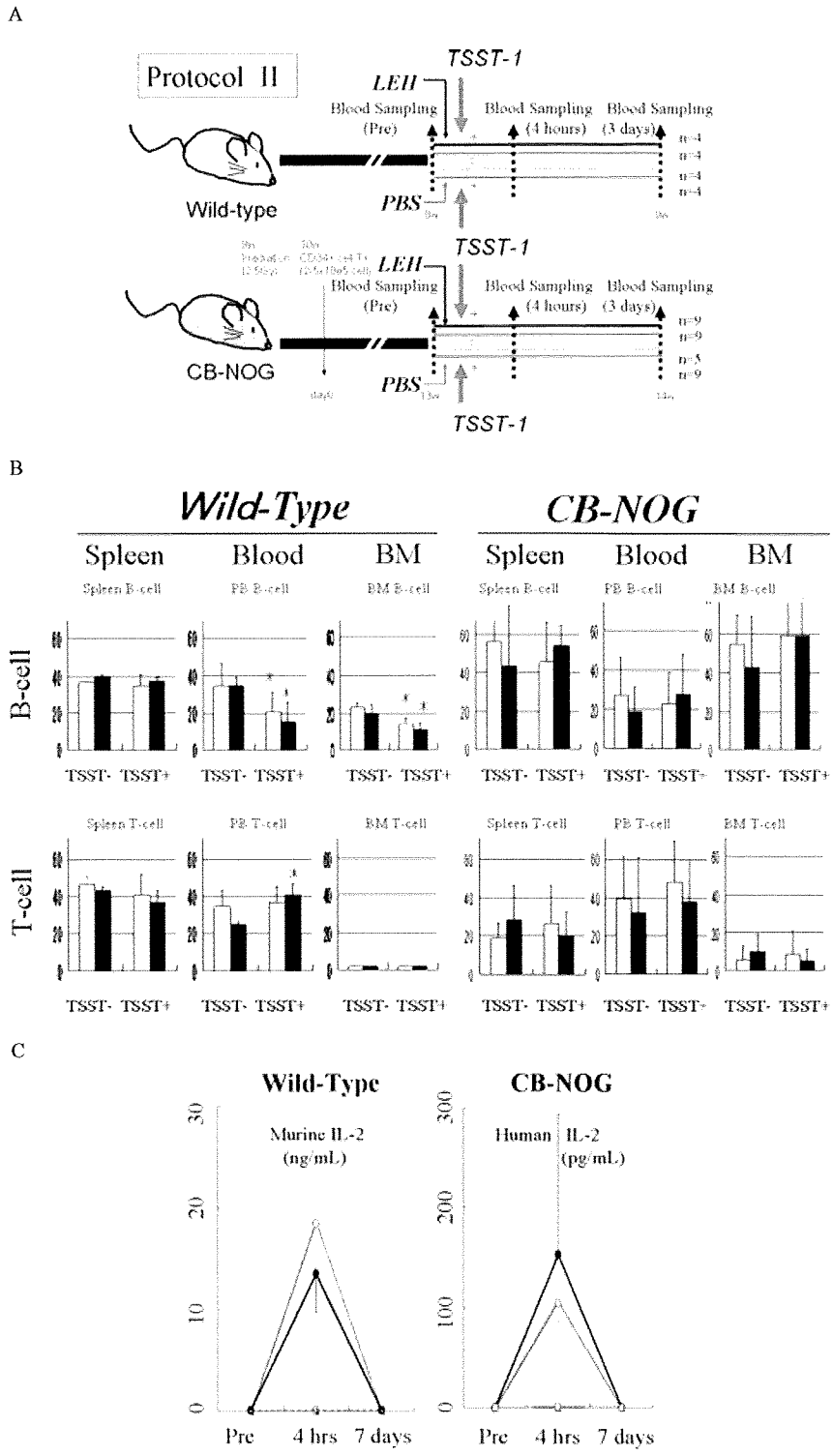

FIG. 3. Immunocompetent cell changes after TSST-1 stimulation. (A) Protocol II: responses to TSST-1 in the presence or absence of LEH. (B) Changes in B-cell and T-cell populations (%) 3 days after administration of LEH (closed columns) or PBS (open columns) with (TSST+) or without TSST-1 stimulation (TSST–) in the spleen (Spleen), peripheral blood (Blood), and bone marrow (BM) in BALB/c (Wild-type) as well as CB-NOG mice (CB-NOG). An asterisk (*) depicts a significant difference between the presence and absence of TSST-1 stimulation. (C) Sequential changes in plasma IL-2 levels in wild-type mice (left panel, murine IL-2) as well as in CB-NOG mice (right panel, human IL-2).

EL. Because of the species difference, wild-type BALB/c mice produced murine IL-2, while CB-NOG mice produced human IL-2. Nonetheless, the level of murine IL-2 was about two orders higher than that of human IL-2 in CB-NOG mice 4 h after TSST-1 administration (Fig. 3C). Because of the larger number of spleen T-cells in BALB/c mice ($200 \pm 27 \times 10^6$) as compared with CB-NOG ($4.1 \pm 2.3 \times 10^6$) 3 days after TSST-1 stimulation, the plasma IL-2 level per 10^6 spleen T-cells was calculated to be equivalent (BALB/c: 70 ± 30 vs. CB-NOG: 32 ± 26 ng/10^6 spleen T-cells), although the timing of determination (IL-2: 4 h, spleen cell number: 3 days after TSST-1 stimulation) was different. Moreover, IL-2 production was not altered by the presence or absence of LEH in either wild-type (LEH+: 70 ± 30 vs. LEH-: 88 ± 66 ng/10^6 spleen T-cells) or CB-NOG mice (LEH+: 32 ± 26 vs. LEH-: 21 ± 24 ng/10^6 spleen T-cells).

Histochemistry

There was no microscopic change in hematoxylin/eosin-stained spleen between animals receiving PBS, EL, or LEH (not shown). The immunohistochemical staining for human T-cells using CD3 and human B-cells using CD20 revealed a regular, scattered, and focal accumulation of these human lymphocytes (not shown). While there was an obvious difference in the immunohistochemical staining for splenic human B-cells (Fig. 4A), as well as T-cells (Fig. 4B) with (TSST+) or without TSST-1 stimulation (TSST–), there was no difference between the presence (LEH) or absence of pretreatment with TRM-645 (PBS).

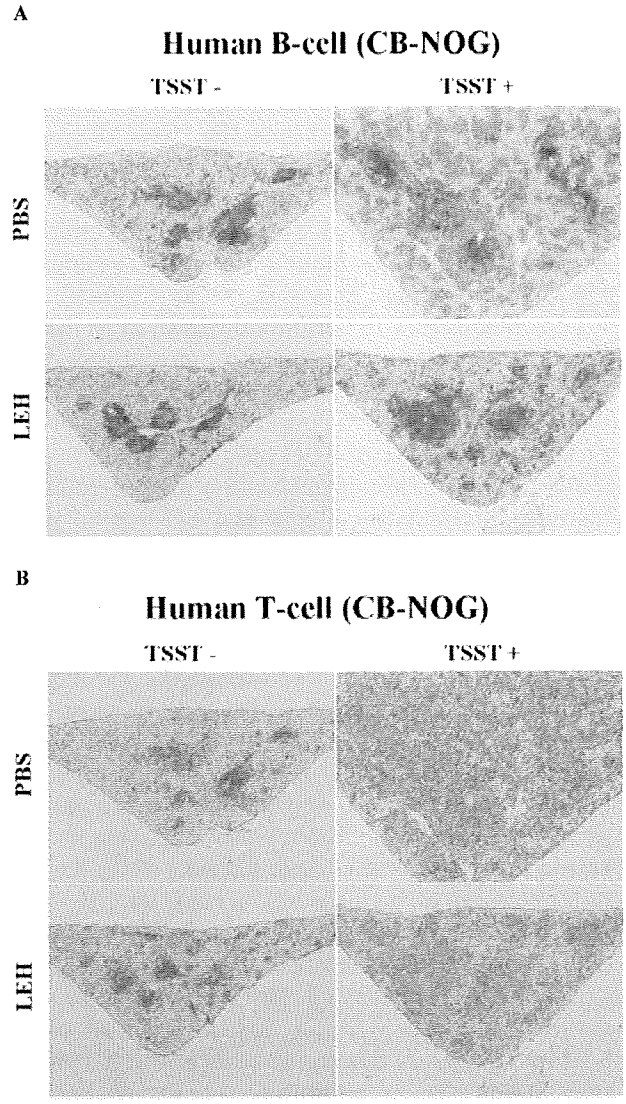

FIG. 4. Immunohistochemical study. A representative immunohistochemical staining of the spleen for human B-cells (A) and T-cells (B) 3 days after pretreatment with saline (PBS) or TRM-645 (LEH) with (TSST+) or without TSST-1 administration (TSST–) in CB-NOG mice.

DISCUSSION

As the safety evaluation in animals does not necessarily equate to human responses, animals with the human immune system are desirable to better serve as a preclinical safety evaluation. Thus, human tissues, including fetal liver, fetal thymus, bone marrow, and lymph nodes, have been used in SCID mouse and NOD-SCID mouse (14). Because of ethical problems, hematopoietic stem cells began to be used instead (15). We developed the CB-NOG mouse (10–14), but found it incomplete as a simulation of the human immune system with regard to the inefficient production of myeloid cells and the lack of antigen-specific human IgG after immunization of conventional antigens. Therefore, we focused on changes in T-cell and B-cell composition and the early reactivity of T-cells to TSST-1 as a surrogate for the human immune response to LEH or TRM-645, as these aspects have been proven to be represented in CB-NOG mice (10–14).

In response to a simple administration of TRM-645 (10 mL/kg), there was no significant or consistent change in lymphocyte composition either in peripheral blood or spleen in wild-type as well as in CB-NOG mice (Protocol I). Since the in vivo half-life of LEH in mice is less than 24 h, infused LEH should have been trapped, eliminated from the circulation, and metabolized in the reticuloendothelial system. Nonetheless, there was no discernible response up to 7 days after administration, although the human

hemoglobin contained in LEH was xenogeneic to wild-type mice and allogeneic to CB-NOG mice. There were some isolated changes after infusion of EL, but they were not associated with the changes observed in LEH-treated mice that were similar to PBS-treated controls. Therefore, EL was not used in the following Protocol II, performed to determine whether the presence of TRM-645 would interfere with the host's active immune response to a superantigen, TSST-1. There was a significant reduction in B-cell composition in peripheral blood, as well as in bone marrow in response to TSST-1 in wild-type mice (Fig. 3B). However, this observation was considered to be insignificant, as it occurred regardless of the presence or absence of LEH only in wild-type, not in CB-NOG mice. The only exception was a significant increase in circulating T-cells in LEH-treated wild-type mice, a phenomenon not seen in saline-treated wild-type controls. This discrepancy was not observed in CB-NOG mice, the only disparate observation between wild-type and CB-NOG mice. As wild-type BALB/c mice are of an inbred strain, the genotype is identical, and the response to a medicine would be uniform. In contrast, CB-NOG mice with a reconstituted human immune system are disparate, as in human individuals. This may account for the heterogeneous reactions in CB-NOG mice, making it difficult to detect possible toxicity because of the variety of human genetic background. In contrast, CB-NOG mice may be useful for detecting toxicity of a medicine that would be consistent in humans but not in experimental animals; an anti-CD28 superagonist antibody developed serious responses in all of six healthy volunteers despite preclinical safety evaluations in animals that allowed the clinical trial (8). In this context, the current observation, a circulating T-cell increase only in wild-type mice but not in CB-NOG mice, may suggest that LEH affects the murine lymphocyte composition, and this is not detectable in the CB-NOG system. Moreover, this observation could have been a reflection of the significant B-cell reduction mentioned before. As only the relative composition between B-cells and T-cells was monitored, such a T-cell increase could have been a result of B-cell reduction or vice versa. This was, in fact, a limitation of the current study. Nonetheless, there was no significant increase in activated T-cell population in any mice (data not shown), suggesting that the increase in T-cell number might have been induced by some additive effects.

The plasma IL-2 level was monitored in the current study because it represents the earliest response of T-cells, unmodified by other preceding responses of natural immunologic processes that are not reproduced in CB-NOG mice. IL-2 levels were elevated 4 h after TSST-1 stimulation by a similar magnitude regardless of the presence or absence of TRM-645 either in wild-type (murine IL-2) or CB-NOG mice (human IL-2), both of which then returned to baseline in 3 days. IL-2 levels stayed at baseline in wild-type mice as well as CB-NOG mice receiving TRM-645 or PBS alone without TSST-1, suggesting that TRM-645 per se did not largely modify or activate T-cells. Although the resultant IL-2 plasma level and its production per spleen T-cells were lower than normal murine T-cells, CB-NOG mice showed patterns similar to those observed in wild-type mice regardless of the presence or absence of LEH in circulation. This could be a simulation of trauma or surgery, when patients lose blood and require RBC supplement under exposure to foreign antigens. In addition, the number of observations was limited, although CB-NOG mice were prepared as human cord blood became available. Although all these factors might have worked for the negative results in Protocol I, the positive and comparable response to TSST-1 in Protocol II works as a positive study, suggesting that the negative results in protocol I originated from the absence of immunogenicity of TRM-645, but not from immunodeficiency of CB-NOG mice.

As LEH is eliminated from the circulation more quickly than RBC because of a short in vivo half-life (4,5), the administration of a larger dose may impose an acute metabolic load of hemoglobin and lipids on the reticuloendothelial system. Therefore, even if LEH itself is immunologically inert, the acute metabolic load on reticuloendothelial cells, phagocytes, and dendritic cells may saturate and competitively inhibit the other metabolic processes, resulting in a relative suppression of any immunologic response to a third-party antigen. While polyethylene glycol on the surface of liposome capsules appeared to suppress the primary immune recognition of TRM-645, responses to repeated administrations need to be addressed, as LEH may be required on multiple occasions in a person, and the secondary exposure may cause adverse and exaggerated immune response(s).

CONCLUSIONS

The results suggest that the administration of LEH (10 mL/kg) per se may not largely affect the immune status (Protocol I) nor interfere with the host's early immune response to bacterial enterotoxins (TSST-1) in murine as well as in human immune systems. Studies on the effects of larger-volume infusions and

repeated administrations are underway. Although the CB-NOG mouse is incomplete at present, it may become useful as a preclinical safety evaluation tool when the system is improved to better mimic the human immune system in the future.

Acknowledgments: This study is supported in part by: New Energy Development Organization; Grant-in-Aid for Scientific Research, B14370365, A16209037, and A20249072 from the Ministry of Education, Culture, Science and Technology, Japan and Research Grant on Human Tissue Engineering (H17-014) from the Ministry of Health, Labor and Welfare, Japan. We acknowledge technical support of Tokai University Teaching and the Research Support Center.

REFERENCES

1. Saxena R, Wijnhoud AD, Carton H, et al. Controlled safety study of a hemoglobin-based oxygen carrier, DCLHb, in acute ischemic stroke. *Stroke* 1999;30:993–6.
2. Nosé Y. Is there a role for blood substitutes in civilian medicine: a drug for emergency shock cases? *Artif Organs* 2004;28:807–12.
3. Ogata Y. Characteristics and function of human hemoglobin vesicles as an oxygen carrier. *Polym Advan Technol* 2000;11: 205–9.
4. Kaneda S, Ishizuka T, Goto H, Kimura T, Inaba K, Kasukawa H. Liposome-encapsulated hemoglobin, TRM-645: current status of the development and important issues for clinical application. *Artif Organs* 2009;33:146–52.
5. Kawaguchi AT, Fukumoto D, Haida M, Ogata Y, Yamano M, Tsukada H. Liposome -encapsulated hemoglobin reduces the size of cerebral infarction in the rat. Evaluation with photochemically induced thrombosis of the middle cerebral artery. *Stroke* 2007;38:1626–32.
6. Kawaguchi AT, Haida M, Yamano M, Ogata Y, Tsukada H. O_2 affinity, dose-response relationship, and long-term effect of artificial O2 carrier after brain ischemia and reperfusion in the primate [Abstract]. *Stroke* 2007;38:599.
7. Chang TM, Lister C, Nishiya T, Varma R. Immunological effects of hemoglobin, encapsulated hemoglobin, and conjugated hemoglobin using different immunization schedules. *Biomat Artif Cell Im* 1992;20:611–8.
8. Suntharalingam G, Perry MR, Ward S, et al. Cytokine storm in a phase 1b trial of the anti-CD28 monoclonal antiboby TGN1412. *N Engl J Med* 2006;355:1018–28.
9. Beyersdorf N, Gaupp S, Balbach K, et al. Selective targeting of regulatory T cells with CD28 superagonists allows effective therapy of experimental autoimmune encephalomyelitis. *J Exp Med* 2005;202:445–55.
10. Matsumura T, Kametani Y, Ando K, et al. Functional CD5+ B cells develop predominantly in the spleen of NOD/SCID/γc^{null} (NOG) mice transplanted either with human umbilical cord blood, bone marrow, or mobilized peripheral blood CD34+ cells. *Exp Hematol* 2003;31:787–97.
11. Saito Y, Kametani Y, Hozumi K, et al. The in vivo development of human T cells from CD34(+) cells in the murine thymic environment. *Int Immunol* 2002;14:1113–24.
12. Ito M, Kobayashi K, Suzue K, et al. NOD/SCID/γc^{null} mouse: an excellent recipient mouse model for engraftment of human cells. *Blood* 2002;100:3175–82.
13. Kametani Y, Shiina M, Katano I, et al. Development of human-human hybridoma from anti-Her-2 peptide-producing B cells in immunized NOG mouse. *Exp Hematol* 2006;34: 1240–8.
14. McCune JM. Development and applications of the SCID-hu mouse model. *Sem Immunol* 1996;8:187–96.
15. Greiner DL, Hesselton RA, Shultz LD. SCID mouse models of human stem cell engraftment. *Stem Cells* 1998;16:166–77.

Immunology
The Journal of cells, molecules, systems and technologies
British Society for immunology

IMMUNOLOGY ORIGINAL ARTICLE

Over-expression of Runx1 transcription factor impairs the development of thymocytes from the double-negative to double-positive stages

Won F. Wong,[1] Megumi Nakazato,[1] Toshio Watanabe,[1*] Kazuyoshi Kohu,[1] Takehiro Ogata,[1] Naomi Yoshida,[1] Yusuke Sotomaru,[2†] Mamoru Ito,[2] Kimi Araki,[3] Janice Telfer,[4] Manabu Fukumoto,[1] Daisuke Suzuki,[5] Takehito Sato,[5] Katsuto Hozumi,[5] Sonoko Habu[5] and Masanobu Satake[1]

[1]*Institute of Development, Aging and Cancer, Graduate School of Life Sciences, Tohoku University, Sendai, Japan,* [2]*Central Laboratory for Experimental Animals, Kawasaki, Japan,* [3]*Institute of Embryology and Genetics, Kumamoto University, Kumamoto, Japan,* [4]*Department of Veterinary and Animal Sciences, Paige Laboratory, University of Massachusetts, Amherst, MA, USA, and* [5]*Department of Immunology, Tokai University School of Medicine, Isehara, Japan*

doi:10.1111/j.1365-2567.2009.03230.x
Received 5 October 2009; revised 17 November 2009; accepted 9 December 2009.
W.F.W. and M.N. contributed equally to the work.
*Present address: Graduate School of Humanities and Biological Sciences, Nara Women's University, 630-8506 Nara, Japan.
†Present address: Natural Science Centre for Basic Research and Development, Hiroshima University, Hiroshima 734-8551, Japan.
Correspondence: Dr M. Satake, Department of Molecular Immunology, Institute of Development, Aging and Cancer, Tohoku University, Seiryo-machi 4-1, Aoba-ku, Sendai, 980-8575, Japan.
Email: satake@idac.tohoku.ac.jp
Senior author: Masanobu Satake

Summary

Runx1 transcription factor is highly expressed at a CD4/CD8-double-negative (DN) stage of thymocyte development but is down-regulated when cells proceed to the double-positive (DP) stage. In the present study, we examined whether the down-regulation of Runx1 is necessary for thymocyte differentiation from the DN to DP stage. When Runx1 was artificially over-expressed in thymocytes by Lck-driven Cre, the DN3 population was unaffected, as exemplified by proper pre-T-cell receptor expression, whereas the DN4 population was perturbed as shown by the decrease in the $CD27^{hi}$ sub-fraction. In parallel, the growth rate of DN4 cells was reduced by half, as measured by bromodeoxyuridine incorporation. These events impaired the transition of DN4 cells to the DP stage, resulting in the drastic reduction of the number of DP thymocytes. The *Runx1* gene has two promoters, a proximal and a distal promoter; and, in thymocytes, endogenous Runx1 was mainly transcribed from the distal promoter. Interestingly, only distal, but not proximal, Runx1 over-expression exhibited an inhibitory effect on thymocyte differentiation, suggesting that the distal Runx1 protein may fulfil a unique function. Our collective results indicate that production of the distal Runx1 protein must be adequately down-regulated for thymocytes to transit from the DN to the DP stage, a critical step in the massive expansion of the T-cell lineage.

Keywords: double negative; double positive; Runx1; thymocyte development; transgenic mice

Introduction

Runx1 and Runx3 transcription factors play critical roles during thymocyte development (see ref. [1] for review). The role of each Runx protein is dependent on its expression pattern during the different stages of thymocyte differentiation. For example, Runx1 protein is produced during the CD4/CD8 double-negative (DN), CD4/CD8 double-positive (DP), CD4 single-positive (SP) and CD8 SP lineages of thymocyte differentiation.[2] Hence, *Lck*-mediated targeting of *Runx1* was reported to cause defects in the differentiation of DN thymocytes, and *CD4*-mediated targeting of *Runx1* disrupted the positive selection of CD4 SP cells.[3,4] On the other hand, Runx3 protein is produced mainly in CD8 SP thymocytes,[2,5] where it suppresses the transcription of *CD4*, a costimulatory molecule of T-cell receptors (TCRs), and that of *ThPok*, a transcription factor specifying the CD4 lineage.[6,7] Runx3 also activates the transcription of *CD8*.[2] Targeting *Runx3* resulted in the abolition of CD8 SP cells in the thymuses of targeted mice.[7]

It is worth noting that a substantial amount of Runx1 protein is expressed at the DN stage, in contrast to the Runx3 protein, which can also be detected but to a lesser extent than Runx1.[2,7,8] In accordance with its expression profile in DN cells, the targeting of *Runx3* had only a marginal effect such as a partial de-repression of CD4 expression,[7,8] whereas a *Runx1* deficiency resulted in severe defects in the differentiation of DN thymocytes. However, the observed defects varied from one report to another, namely the developmental block at either the DN1 to DN2, DN2 to DN3, or DN3 to DN4 stages of differentiation.[3,4,9] This variation may be the result of the different targeting methods used, for example, the use of different promoter-driven *Cre*-transgenic mice. In any case, the targeting studies established clearly that Runx1 is essential for the correct differentiation of DN thymocytes.

Expression of the *Runx1* gene is initiated from two distinct promoters, distal and proximal.[10,11] In thymocytes, the majority of *Runx1* transcripts represent transcription from the distal promoter.[12] Distal and proximal *Runx1* transcripts encode Runx1 proteins that are identical except for the last 19 amino acid residues (in the distal isoform) and the last five amino acids (of the proximal isoform), at the N-terminal end of the protein. Runx1 protein (mainly the distal isoform) is detected throughout the stages of thymocyte differentiation. Its level of expression is highest at the DN stage, and it is then substantially down-regulated at the DP stage.[2] This down-regulation of the Runx1 protein occurs in parallel with changes in *Runx1* transcripts.[7] The implications of this phenomenon are unknown. The studies cited above used a gene knockout approach to evaluate the significance of Runx1 protein expression in the DN subset, but provided no explanations for the possible consequences of Runx1 down-regulation.

In the present study, we focused on the issue of whether the down-regulation of Runx1 protein is a necessary step in the correct progression of thymocytes from the DN to the DP stage. For this purpose, transgenic Runx1 was artificially over-expressed in thymocytes, with the expectation that it would disturb the physiological down-regulation of Runx1. We observed that the over-expressed Runx1 protein is an inhibitory factor during the DN to DP transition. Interestingly, this inhibitory effect was observed only with over-expression of the distal isoform, but not the proximal isoform, suggesting that this effect was unique to the distal isoform of the Runx1 transcription factor.

Materials and methods

Cell culture

The three T-cell lines EL-4, TK-1 and 1200M, and MEL cells (an erythroleukaemic cell line) were grown in RPMI-1640 medium (Gibco/Invitrogen, Carlsbad, CA), whereas NIH3T3 fibroblasts were cultured in Dulbecco's modified Eagle's medium. Both media were supplemented with 10% [volume/volume (v/v)] fetal bovine serum (FBS).

Plasmids

The plasmids *dRunx1-HA* and *pRunx1-HA* representing the murine *Runx1* coding region of the distal (d) and proximal (p) isoforms, respectively, each contained a haemagglutinin (HA) tag fused to the C-terminal of Runx1. A *Bgl*II–*Eco*RI fragment harbouring *Runx1-HA* was cleaved from each plasmid and cloned into the *Eco*RV site of the plasmid *pCAG-CAT-oligo*. This *CAT* (chloramphenicol acetyltransferase) plasmid harbours a *CAG* (chicken β-actin) promoter-driven *CAT-SV40pA* element flanked by *loxP* sites.[13] The resulting plasmids were designated as *pCAG-loxP-CAT-loxP-dRunx1-HA* and *pCAG-loxP-CAT-loxP-pRunx1-HA*, respectively.

Mice

A *Kpn*I–*Not* I fragment containing *pCAG-loxP-CAT-loxP-Runx1-HA* was purified and microinjected into fertilized eggs from C57BL/6 mice. Transgenic founders were identified and crossed to C57BL/6 mice. The presence, or absence, of the transgene was examined by polymerase chain reaction (PCR) using genomic DNA as a template. The sense and antisense primers were as follows: for *dRunx1*, 5′-ATGGCTTCAGACAGCATTTTTGAG-3′ and 5′-ATGCGTATCCCCGTAGATGCC-3′; for *pRunx1*, 5′-TCCCCCGGGCTTGGTCTGATCATC-3′ and 5′-ATGC

GTATCCCCGTAGATGCC-3′, respectively. *Proximal Lck-Cre*-transgenic mice were provided by J. Takeda.[14]

Flow cytometry

Cells were liberated from the mouse thymus and suspended in phosphate-buffered saline (PBS) containing 1% (v/v) FBS. Cell surface proteins were labelled by incubating single-cell suspensions of 2×10^6 cells with appropriately diluted monoclonal antibodies (mAbs) on ice for 30 min. Intracytoplasmic proteins were labelled by fixing and permeabilizing the surface-labelled cells using a FIX & PERM kit (Caltag Laboratories, Burlingame, CA), followed by incubation with a second mAb on ice for 30 min. The following fluorescein-conjugated mAbs were used: fluorescein isothiocyanate- (FITC-) Thy-1.2, FITC-TCR-β, FITC-CD3ε, FITC-CD25, FITC-HSA (heat stable antigen), FITC-Annexin V, phycoerythrin- (PE-) CD8a, PE-CD44, PE-CD25, PE-CD27, PE-TCR-γδ, Cychrome-CD4, Cychrome-CD8a, Cychrome-CD44 (these 14 mAbs were from BD Pharmingen, San Jose, CA), RED613-CD4 and RED613-CD8a (these two mAbs were from GibcoBRL, Gaithersburg, MD). The labelled cells were separated with an analytical EPICS-XL flow cytometer (Beckman Coulter, Miami, FL), and the data were analysed with EXPO32 software (Beckman Coulter).

Fractionation of thymocytes

Various thymocyte subsets were purified from a total thymocyte suspension using Auto-MACS (Miltenyi Biotech GmbH, Bergisch Gladbach, Germany) or FACStar (Becton Dickinson, Mountain View, CA). The subsets prepared in this way corresponded to DN1/2, DN3, DN4 and DP fractions. The DN3 was further sub-divided into DN3S and DN3L based on cell size. The purity of each isolated fraction was > 95% as judged by flow cytometry.

Immunoblot analysis

Protein was extracted from 1×10^6 cells and dissolved in 80 μl of 9 M urea, 2% (v/v) Triton-X-100, 1% [weight/volume (w/v)] dithiothreitol and 20 μl of 10% (w/v) lithium dodecylsulphate. Protein extract, equivalent to 2×10^5 cells, was loaded in one lane, separated through a sodium dodecyl sulphate 8% (w/v) polyacrylamide gel, and electroblotted on to a polyvinylidene difluoride (PVDF) membrane (BioRad, Hercules, CA). The filter was blocked by immersing it in PBS containing 5% (w/v) skimmed milk at 4° overnight. The primary antibodies used were anti-HA mAb 3F10 (Roche Diagnostics, Indianapolis, IN), anti-β-actin mAb (Santa Cruz Biotechnology, Santa Cruz, CA) or anti-panRunx-peptide rabbit serum.[15] Anti-rat immunoglobulin G or anti-rabbit immunoglobulin G were used as the secondary antibodies. Immunocomplexes were detected using an ABC kit (Vector Laboratories, Burlingame, CA) and exposed to X-ray film (Fujifilm, Tokyo, Japan).

Southern blot analysis

Genomic DNA was prepared from the tails of mice by proteinase K digestion, phenol–chloroform extraction and ethanol precipitation. DNA was digested with *Eco*RI, electrophoresed through a 0·8% (w/v) agarose gel and processed for Southern blot analysis as described previously.[16] The hybridization probe contained the Runt domain sequence of murine *Runx1* complementary DNA (cDNA).

Reverse transcription–polymerase chain reaction analysis

RNA was extracted from cells using Isogen (Nippon Gene, Tokyo, Japan) and cDNA was synthesized from RNA using Superscript II reverse transcriptase (Invitrogen, Carlsbad, CA). The PCR amplification was performed for 25 cycles using a cDNA template and LA-*Taq* polymerase (Takara, Ohtsu, Japan). The following sense and anti-sense primers were used to detect transcripts: for *distal Runx1*, 5′–ATGGCTTCAGACAGCATTTTTGAGTCATTT–3′ and 5′–ACTGTCATTTTGATGGCTCTATGGTAGGT–3′; for *proximal Runx1*, 5′–ATGCGTATCCCCGTAGATGCCAGCAC–3′, and 5′–ACTGTCATTTTGATGGCTCTATGGTAGGT–3′; for *β-actin*, 5′–GATGACGATATCGCTGCGCTG–3′ and 5′–GTACGACCAGAGGCATACAGG–3′; and for *pTα*, 5′-TCACACTGCTGGTAGATGGAAGG-3′ and 5′-CATCGAGCAGAAGCAGTTTGA-3′.

Northern blot analysis

Poly(A)$^+$ RNA was selected from the RNA fraction using Oligo-dT-Latex (Takara), and 2 μg was separated on a 1% (w/v) agarose gel containing 2·2 M formaldehyde. Electronic transfer, hybridization and washing procedures were as described previously.[17] Specific *distal* or *proximal Runx1* probes corresponding to 5′ untranslated regions of each *Runx1* transcript were radioactively labelled and used for detection of each *Runx1*. Sequences of each probe were as follows: for *proximal Runx1*, 5′-CGCATCACAA CAAGCCGATTGAGTAAGGACCCTGAAAACAGCTCCTA CTAGACGGCGACAGGGGCTCGGATCTTCTGCAAGCT GCTCCCGGGAGACCAACATACAAGTTCAGAAGCCTT TATTACTACCGGAGGGTTGTGGGGGTAGGAGACTAA ATTACCATCAGTCCCGGACTGAGATCTAGTTACACG GA&CGCATCACAACAAGCCGATTGAGTAAGGACCCT-GAAAACAGCTCCTACTAGACGGCGACAGGGGCTCGG-ATCTTCTGCAAGCTGCTCCCGGGA CGCA-3′, and for *distal Runx1*, 5′-AAACAACCACAGAACCACAAGTTGGT-AGCCTGGCAGTGTCAGAAGTGTAAGCCCAGCACAGT-GGTCAGCAGGCAGGACGAATCACACTGAATGCAAAC

CACAGGCTTTCGCAGAGCGGTGAAAGAAATTATAGA-ATCCCCCGCCTTCAGGTAGTAGGTGCGTTTTCGAAA GGAAACGATGGCTTCAGACAGCAÛAAACAACCACAG-AACCACAAGTTGGTAGCCTGGCAGTGT-3′.

Detection of TCR-β recombination

A DN3 thymocyte subset was purified as described above, and genomic DNA was prepared from cells using Isogen. The frequency of *DJ* and/or *V(D)J* recombination was evaluated by PCR amplification using specific primers and 6·25 ng, 25 ng and 100 ng of genomic DNA as templates. The PCR cycle numbers were 28 for *Rag2*, 30 for *DJ* recombination and 33 for *V(D)J* recombination. The PCR products were separated on agarose gels and electroblotted onto PVDF membranes. The filters were processed for Southern blot hybridization using specific oligonucleotides as labelled probes. The sequences of the PCR primers and those of the oligonucleotide probes were as described previously.[18,19] Specifically, table 1 in ref. [19] is convenient to find the sequences. Recombination detected represented Dβ2-Jβ2, Vβ2-Jβ2, Vβ4-Jβ2, Vβ10-Jβ2 and Vβ14-Jβ2, respectively.

Bromodeoxyuridine labelling of cells

One milligram of 5-bromo-2-deoxyuridine (BrdU) in PBS was injected intraperitoneally into a mouse, and the thymus was excised after 4 hr. Cell surface proteins were fluorescently labelled as described above, and the cells with incorporated BrdU were then detected using a BrdU Flow Kit (BD Biosciences, San Diego, CA). Briefly, 2×10^6 cells were fixed, permeabilized, digested with 300 μg/ml DNAse I in PBS for 1 hr at 37°, and incubated with FITC-anti-BrdU for 20 min in the dark. Labelled cells were analysed by flow cytometry as described above.

Results

Expression of Runx1 transcript and protein decreases accompanying the DN to DP differentiation of thymocytes

We first examined the expression profiles of *Runx1* transcript by semi-quantitative reverse transcription (RT-) PCR analysis (Fig. 1a). The DN as well as DP fractions were prepared from thymuses of C57BL/6 mice. The DN fraction was further sub-divided into DN1/2, DN3 and DN4, using CD25 and CD44 as fractionation markers. DN3S ($CD44^-$ $CD25^{hi}$, small) and DN3L ($CD44^-$ $CD25^{low}$, large) represent sub-fractions of DN3 before and after pre-TCR mediated selection. The amount of *distal Runx1* transcript was maximal at the DN3S stage and decreased markedly at the subsequent stages such as DN3L, DN4 and DP. We note that, when primers specific

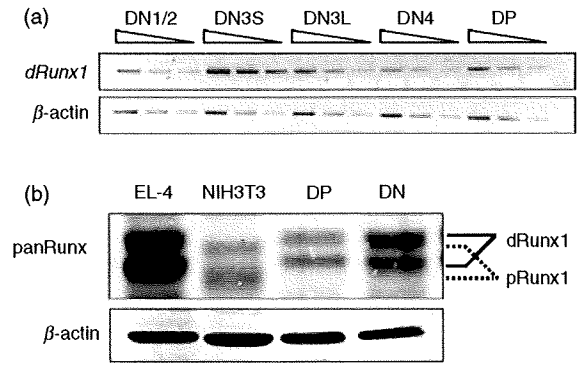

Figure 1. Expression profiles of Runx1 transcript and protein in the double-negative (DN) and double-positive (DP) fractions prepared from thymocytes of wild-type C57BL/6 mice. (a) Semi-quantitative reverse transcription–polymerase chain reaction (RT-PCR) analysis of *distal Runx1* transcript levels during thymocyte differentiation. RNA was extracted from DN1/2, DN3S, DN3L, DN4 and DP fractions each, and converted to complementary DNAs (cDNA). An increasing amount of cDNA was used for PCR as indicated. Transcript of *β-actin* served as a control. (b) Immunoblot analysis of Runx1 protein in thymocytes. Protein extracts were prepared from the DN and DP fractions as well as from EL-4 and NIH3T3 cell lines, and processed for immunoblot detection using anti-panRunx antibody. A slight but significant difference in the migration corresponded to distal and proximal Runx1 polypeptides as indicated. β-actin served as a loading control.

to proximal *Runx1* transcript were used, PCR products were detected only after extensive cycles of amplification (data not shown). This is in accordance with the literature describing scarce expression of proximal *Runx1* in thymocytes.[12]

Figure 1(b) shows immunoblot analysis of DN and DP cells, using anti-panRunx antibody. The detected doublet bands of Runx1 corresponded to unphosphorylated and phosphorylated forms, as reported.[20] In agreement with the result of the RT-PCR, the amount of Runx1 protein was higher at the DN stage and decreased at the DP stage. To confirm which of the distal and proximal Runx1 proteins was expressed in thymocytes, lysates were prepared from EL-4 and NIH3T3 cells and probed in parallel, because these cell lines expressed solely *distal* or *proximal Runx1* transcripts, respectively (Fig. S1). As expected, doublets detected for thymocytes co-migrated with doublets in EL-4 that corresponded to *distal Runx1*. Taking the above findings together, levels of *distal Runx1* transcript and protein were high at the DN stage (DN3S) and decreased at the DP stage of thymocytes.

Establishment of *Runx1*-transgenic mouse lines

The purpose of this study was to elucidate the functional significance of the Runx1 down-regulation that accompanies the differentiation of thymocytes from the DN to DP stages. We tried to counter the Runx1 down-regulation

by artificially over-expressing *distal* or *proximal Runx1* and examining its effect on thymocyte differentiation. We generated transgenic (tg) mice that harboured *pCAG-loxP-CAT-loxP-Runx1-HA* in the genome (Fig. 2a, upper). To screen for a positive mouse line, genomic DNA extracted from the tails of mice was prepared for Southern blot analysis (Fig. 2b). A probe recognizing the *Runt* domain of *Runx1* was used for detection of the transgene (indicated by arrows) as well as the endogenous gene (arrowheads). We managed to establish four lines of transgenic mice, including lines 2 and 31 harbouring *distal Runx1-tg* and lines 32 and 55 harbouring *proximal Runx1-tg*.

Runx1-HA was not expressed in *Runx1-tg* mice because the transcription of *Runx1* from the *CAG* promoter was hindered by the presence of the *CAT* gene and the *SV40*-derived poly A (pA) addition element (Fig. 2a, upper). We then crossed *Runx1-tg* mice with *Lck-Cre-tg* mice. In the T lymphocytes of *Runx1-tg;Lck-Cre-tg* double-transgenic mice, the *CAT-SV40pA* element was cleaved off by *Lck*-driven Cre recombinase, permitting the *CAG* (chicken β-actin, not *Lck*) promoter to drive the expression of *Runx1-HA* (Fig. 2a, lower part). Protein extract was prepared from the thymuses of the transgenic mice and processed for immunoblot analysis using an anti-HA antibody (Fig. 2c). *Runx1-HA*-positive bands were not detected in the single-transgenic *Runx1-tg* thymocytes (left-hand column), but were evident in the thymocytes from the *Runx1-HA-tg;Lck-Cre-tg* double-transgenic animals (right-hand column).

Essentially similar thymocyte phenotypes were obtained from the two distal mouse lines (2 and 31) and the two proximal mouse lines (32 and 55) so the results obtained from lines 2 and 32 are shown as being representative. First, an extent of Runx1 over-expression was evaluated for these two lines (Fig. 2d). The DN fractions were purified from *Lck-Cre-tg*, *distal Runx1-tg;Lck-Cre-tg* and *proximal Runx1-tg;Lck-Cre-tg* thymuses, respectively, and processed for immunoblot analyses using anti-panRunx antibody. Levels of Runx1 protein were 1·4-fold increased in both types of *Runx1-tg* cells as compared with the non-*Runx1-tg* cells. This confirmed the additive expression of transgene-derived protein.

Over-expression of *distal*, but not *proximal*, *Runx1* reduces the number of thymocytes

We observed that the macroscopic size of the thymus from *distal Runx1-tg;Lck-Cre-tg* mouse was much smaller than that from *Lck-Cre-tg* mouse (Fig. 3a). The total number of thymocytes in the *distal Runx1-tg;Lck-Cre-tg* mice (closed box) was reduced to one-ninth of that in the *Lck-Cre-tg* mice (open box), whereas the total number of thymocytes in the *proximal Runx1-tg;Lck-Cre-tg* (shaded box) was not affected ($n = 3$ for each genotype).

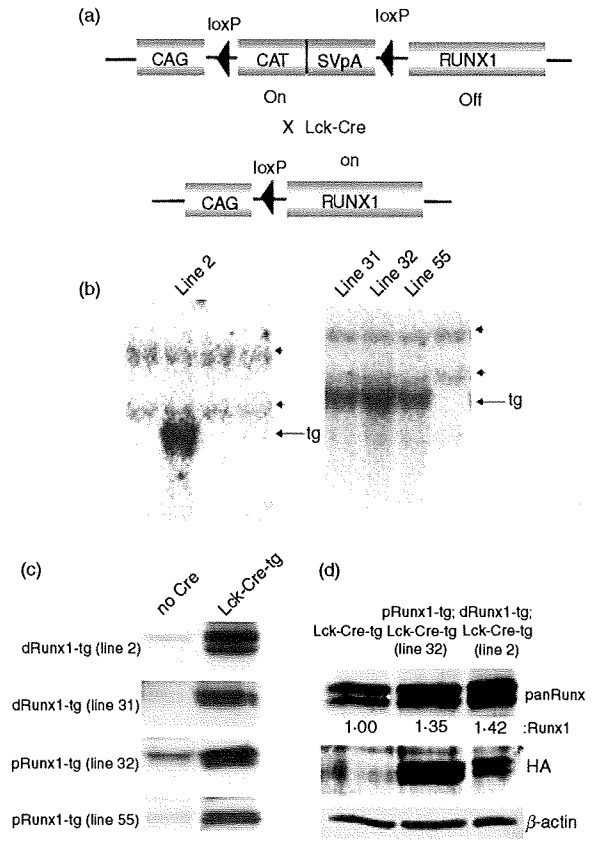

Figure 2. Establishment of *Runx1* transgenic mouse lines. (a) Schematic illustration of the *Runx1*-transgene in the mouse genome. In a *Runx1* single-transgenic mouse (upper), the *CAG* promoter-driven transcript of the *CAT* gene is polyadenylated by an *SV40pA* element, hence impeding *Runx1* expression. On the other hand, in a *Runx1* and *Cre* double-transgenic mouse (lower), the *CAT-SV40pA* element is deleted, so allowing *CAG* promoter-driven expression of *Runx1*. (b) Detection of the *Runx1*-transgene by Southern blot analysis. Genomic DNAs were prepared from each mouse line, digested by *Eco*RI and processed for Southern blot analysis using the *Runt* domain of *Runx1* as a hybridization probe. Arrows and arrowheads indicate the *Runx1* transgene and endogenous *Runx1* gene, respectively. Lines 2 and 31 harbour *distal Runx1*, whereas lines 32 and 55 harbour the *proximal Runx1* isoform. (c) Detection of transgene-derived Runx1-haemagglutinin (HA) protein by immunoblot analysis. Protein extracts were prepared from thymocytes and processed for immunoblot detection using an anti-HA antibody. The left-hand column indicated by '*no Cre*' represents *Runx1* single *tg* mice, whereas the right-hand column indicated by '*Lck-Cre-tg*' represents *Runx1;Lck-Cre* double *tg* mice. *dRunx1* and *pRunx1* denote *distal* and *proximal Runx1*, respectively. (d) Immunoblot detection of Runx1 protein expressed in the double-negative (DN) thymocytes. The DN fractions were purified from *Lck-Cre-tg*, *distal Runx1-tg;Lck-Cre-tg* (line 2) and *proximal Runx1-tg;Lck-Cre-tg* (line 32) thymuses, respectively, and cell lysates were processed for immunoblot using anti-panRunx, anti-HA and anti-β-actin antibodies each. Levels of Runx1 protein were quantified by a densitometer, and presented as the ratios relative to that in the *Lck-Cre-tg* cells as 1.00.

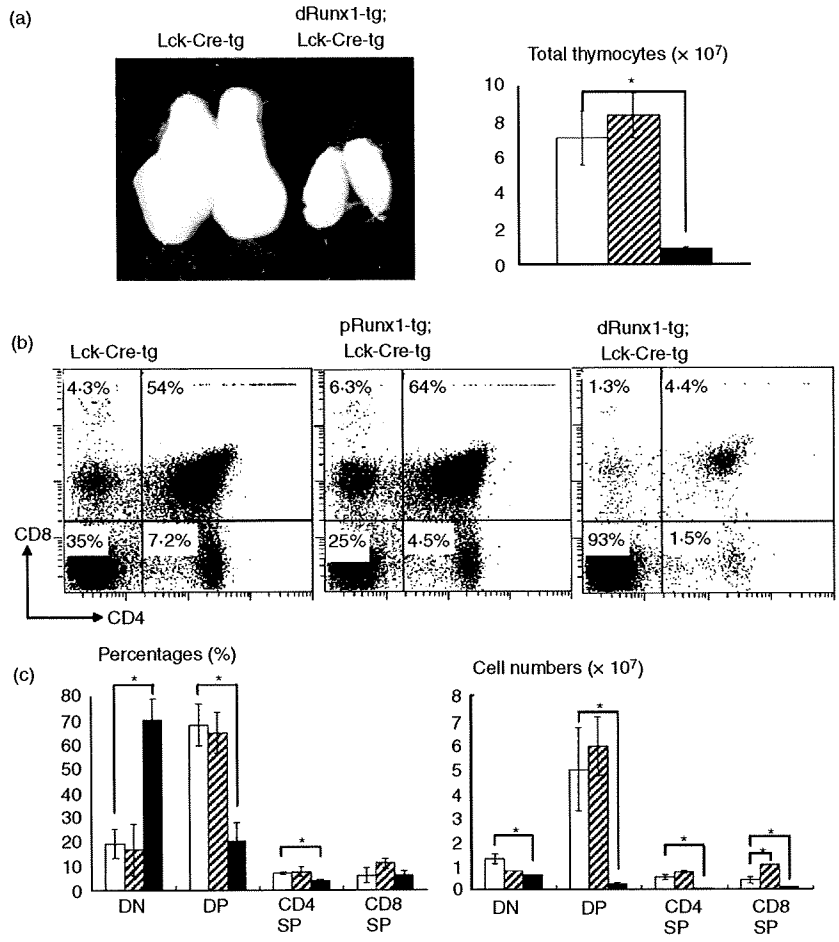

Figure 3. Effects of *Lck*-driven *Runx1* over-expression on thymocyte differentiation. (a) Gross appearance of thymuses and total numbers of thymocytes. (b) Thymocytes were isolated from the transgenic mice indicated and processed for the flow cytometric analysis of CD4 and CD8 expression. Numbers given in each quadrant indicate the percentages of cells in each subset. Representative profiles are shown here. (c) Comparison of the percentages and cell numbers of double-negative (DN), double-positive (DP), CD4 single-positive (SP) and CD8 SP subset. In (a) and (c), the genotypes of mice were *Lck-Cre-tg* (open bars), *proximal Runx1-tg;Lck-Cre-tg* (shaded bars) and *distal Runx1-tg;Lck-Cre-tg* (closed bars), respectively. Mean ± SD ($n = 3$) are shown for each thymocyte subset and each transgenic mouse. Significances of difference were statistically tested by Student's *t*-test, and if detected between the compared genotypes, they are indicated by brackets with *($P < 0{\cdot}05$). (b) CD4 repression by Runx1 over-expression was not observed in the present study, unlike the case of Runx1 introduction into a thymocyte culture by retrovirus.[37] (c) The number of CD8 SP cells was significantly increased in *proximal Runx1-tg;Lck-Cre-tg* compared with *Lck-Cre-tg* thymuses ($P < 0{\cdot}05$). This observation supports our previous report of *CD2*-driven, *proximal Runx1-tg* thymuses.[5]

In Fig. 3(a), statistical significance of difference was tested using Student's *t*-test, and is indicated, if any, by an asterisk ($P < 0{\cdot}05$).

To examine the effect of *Runx1* over-expression, we performed flow cytometric analysis of CD4 and CD8 expression in thymocytes (Fig. 3b). As the thymocytes of *Lck-Cre-tg* mice contained an unusually high proportion of DN cells (20% on average) compared with a wild-type thymus (around 5%, data not shown), we used the *Lck-Cre-tg* mice as controls throughout this study when analysing *Runx1-tg;Lck-Cre-tg* thymuses. A remarkable difference in the DP fractions was observed between the *distal Runx1-tg;Lck-Cre-tg* and control mice. The proportion of DP cells was dramatically reduced in the *distal Runx1-tg;Lck-Cre-tg* thymus compared with the single *Lck-Cre-tg* thymus (4·4% compared to 54%). Additionally, the percentages of CD4 SP and CD8 SP cells were also significantly lower in the *distal Runx1-tg;Lck-Cre-tg* thymus (1·5% and 1·3%, respectively) compared with the *Lck-Cre-tg* thymus (7·2% and 4·3%, respectively).

From the analysis of the absolute cell counts (Fig. 3c), we found that in the *distal Runx1-tg;Lck-Cre-tg* thymus, the reduction in the total number of thymocytes (Fig. 3a) was mainly the result of the massive reduction in the number of DP cells (Fig. 3c). Although the percentage of DN cells increased substantially in the *distal Runx1-tg;Lck-Cre-tg* thymus, the actual number of DN cells decreased to half that of the control. It is therefore likely that over-expression of *distal Runx1* impairs the DN to DP transition. In contrast to the results from *distal Runx1-tg;Lck-Cre-tg*, the percentages of each DN and DP subset were fairly similar between *proximal Runx1-tg;Lck-Cre-tg* and the control *Lck-Cre-tg* thymuses.

DN differentiation is perturbed in the *distal Runx1-tg;Lck-Cre-tg* thymocytes

To characterize the DN cells in more detail, we performed three-colour flow cytometric analysis of CD4, CD8 and Thy-1.2, and found that the ratios of Thy-1.2-positive versus Thy-1.2-negative DN cells were similar in the *Runx1-tg* and control thymuses. Furthermore, the Thy1.2$^+$-gated fraction demonstrated proportions of DN, DP and SP subtypes that were essentially identical to those of non-gated thymocytes (Fig. S2). We also examined TCR-$\gamma\delta$ expression and found that the percentages of TCR-$\gamma\delta^+$

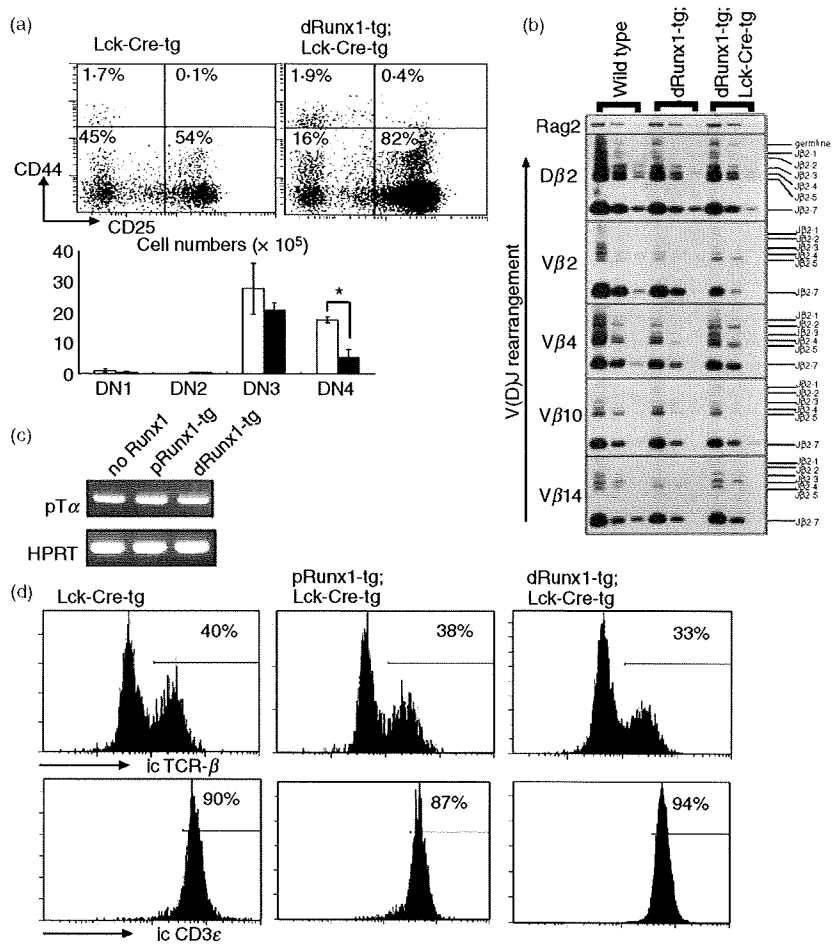

Figure 4. Effects of *Lck*-driven *Runx1* over-expression on double-negative (DN) thymocyte differentiation. (a) Sub-staging of DN thymocyte differentiation. Thymocytes from *distal Runx1-tg;Lck-Cre-tg* (closed bars) and *Lck-Cre-tg* mice (open bars) were processed for flow cytometric analysis of CD4/CD8, Thy-1.2, CD44 and CD25. The data shown here were gated for the Thy-1.2$^+$ CD4$^-$ CD8$^-$ fraction that represents authentic, DN T lymphocytes. Sub-staging of DN cells was based on the levels of CD44 and CD25 expression. The representative expression profiles are shown as well as the mean ± SD values (n = 3) of the absolute number of cells at each DN sub-stage. Significances of difference were statistically tested by Student's t-test, and if detected between the compared genotypes, they are indicated by a bracket with *($P < 0{\cdot}05$). (b) Detection of *TCRβ* gene recombination in DN thymocytes. The DN3 subset of cells was purified by cell-sorting from C57BL/6 (wild-type), *distal Runx1-tg* and *distal Runx1-tg;Lck-Cre-tg* mice, and genomic DNA was prepared. Polymerase chain reaction (PCR) was performed using different amounts of template DNA and specific oligonucleotides as primers. PCR products were processed for Southern blot analysis. The patterns of *V(D)J* recombination detected are as indicated. *Rag2* served as a control. (c) Expression of *pTα* in thymocytes. RNA was prepared from total thymocytes, and processed for reverse transcription-PCR. Transcripts representing *pTα* and *HPRT* were amplified. (d) DN3 subset was purified from thymocytes, stained for intracytoplasmic T-cell receptor-β (TCR-β) and CD3ε and processed for flow cytometric analysis. Numbers indicate the proportions of TCR-β$^+$ and CD3ε$^+$ cells in each DN3 subset.

cells in the DN fractions were similarly low in both *Lck-Cre-tg* and *distal Runx1-tg;Lck-Cre-tg* thymuses (Fig. S3a). These results confirm that the DN cells, illustrated in Fig. 3, mostly reflect authentic T lymphocytes of αβ lineage.

The DN population can be subdivided into four sub-stages designated as DN1 (CD44$^+$ CD25$^-$), DN2 (CD44$^+$ CD25$^+$), DN3 (CD44$^-$ CD25$^+$) and DN4 (CD44$^-$ CD25$^-$). To examine the differentiation of DN cells, we carried out four-colour flow cytometric analysis using CD4/CD8, Thy-1.2, CD44 and CD25. The CD44 and CD25 expression profiles of the Thy-1.2$^+$-gated DN fractions are shown in Fig. 4(a). In the *distal Runx1-tg;Lck-Cre-tg* thymus, the percentages of DN1 and DN2 cells were normal. However, the percentages of DN3 and DN4 cells were increased and decreased, respectively, compared with the *Lck-Cre-tg* thymus. When the absolute cell number of each DN subset was counted, the DN4, but not DN3, cell numbers were substantially decreased in the *distal Runx1-tg;Lck-Cre-tg* thymus. This suggests that over-expression of *distal Runx1* probably causes a defect at the DN4 rather than the DN3 stage.

Pre-TCR expression proceeds appropriately in the *distal Runx1-tg;Lck-Cre-tg* thymocytes

The DN3 stage is a critical step in early thymocyte differentiation as *DJ* and *V(D)J* rearrangements take place at this stage to form the pre-TCR complex.[21] Cells that fail to form a functional pre-TCR die by apoptosis. We investigated whether pre-TCR expression proceeded correctly in the *distal Runx1-tg;Lck-Cre-tg* cells. Genomic DNA was prepared from the purified DN3 fraction and used as a template for PCR amplification. Specific PCR primers and hybridization probes were designed to detect various patterns of *DJ* and *V(D)J* segment recombination.[18,19] As far as the gene combinations examined were concerned, the *DJ* and *V(D)J* segments of *TCRβ* were properly rearranged in the DN3 cells from *distal Runx1-tg;Lck-Cre-tg*, *distal Runx1-tg* and wild-type thymuses (Fig. 4b).

The expression of the pre-TCR complex itself was also examined. The major components of the pre-TCR complex include pTα, TCR-β and CD3ε. Transcripts of *pTα* were detected in thymocytes from *distal Runx1-tg;Lck-Cre-tg* mice (Fig. 4c) and intracytoplasmic TCR-β and CD3ε expression was detected by flow cytometric analysis (Fig. 4d). Both TCR-β and CD3ε were expressed to a similar extent in DN3 thymocytes from the *distal Runx1-tg;Lck-Cre-tg*, *proximal Runx1-tg;Lck-Cre-tg* and *Lck-Cre-tg* mice. Based on the observations illustrated in Fig. 4, it is not likely that over-expression of *distal Runx1* affects the process of pre-TCR expression at the DN3 stage.

DN4 differentiation as probed by CD27-expression is impaired in the *distal Runx1-tg;Lck-Cre-tg* thymocytes

We then examined the differentiation status of DN thymocytes using other markers such as HSA (Fig. 5a) and CD27 (Fig. 5b). In non-gated, *distal Runx1-tg;Lck-Cre-tg* thymocytes, a substantial peak of HSA^{hi} population was observed in addition to an HSA^{lo} population. Furthermore, mean fluorescence intensity of HSA in the DN fraction was higher in the *distal Runx1-tg;Lck-Cre-tg* compared with that in the *Lck-Cre-tg* (217 versus 122). This suggests that the majority of the *distal Runx1-tg;Lck-Cre-tg* DN cells were highly immature.

CD27 is a newly reported DN marker whose expression is low at the DN3S stage ($CD27^{lo}$) and increases sharply at the DN3L ($CD27^{med}$) and DN4 stages ($CD27^{hi}$).[22] Although the DN1/2 cells also express high CD27, they constitute < 3% of the entire DN population, and contribute little to the $CD27^{med/hi}$ population. These $CD27^{med}$ and $CD27^{hi}$ populations were substantially increased and decreased, respectively, in the DN fraction from *distal Runx1-tg;Lck-Cre-tg* thymus (43% and 57% each) compared with those from *Lck-Cre-tg* thymus (29% and 71% each). Alteration of CD27 expression pattern was analogous to the CD25 and CD44 profile in the sense that the

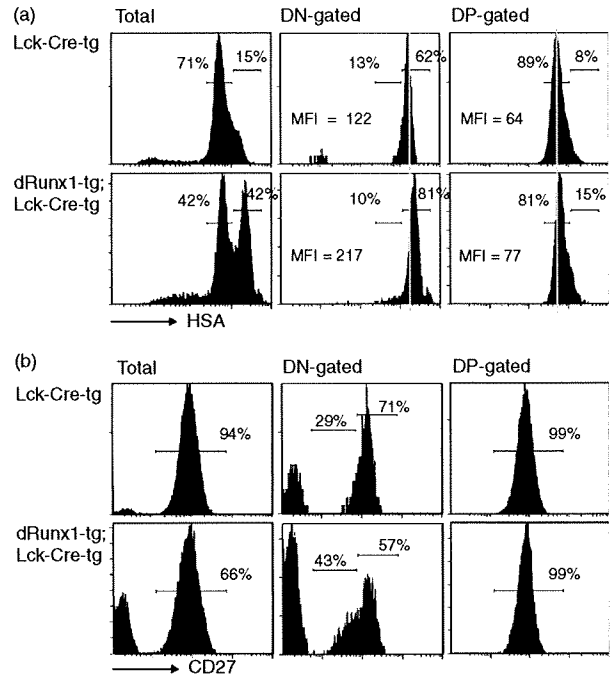

Figure 5. Flow cytometric analyses of HSA/CD27 expression in the double-negative (DN) and double-positive (DP) fractions. Thymocytes were prepared from *Lck-Cre-tg* and *distal Runx1-tg;Lck-Cre-tg* mice, and processed for flow cytometric analyses of CD4, CD8 and HSA/CD27. The DN-gated and DP-gated fractions were analysed for their fluorescence intensities of HSA (a) and CD27 (b). In (a), the percentages of HSA^{hi} and HSA^{lo} sub-fractions and the mean fluorescence intensities of HSA are indicated, whereas the numbers seen in (b) indicate the percentages of $CD27^{med/hi}$ sub-fractions. Note that the percentage of $CD27^{med/hi}$ is assumed to be 100 for the DN fractions in (b).

percentage of DN3 increased and that of DN4 decreased in the DN cells from *distal Runx1-tg;Lck-Cre-tg* thymus (see flow cytometry analyses in Fig. 4a). Collectively, the alterations of HSA and CD27 expressions observed in the *distal Runx1-tg;Lck-Cre-tg* thymocytes suggest an impairment of thymocyte differentiation at the DN3L/DN4 stage.

Over-expression of *distal Runx1* reduces the growth activity of thymocytes at the DN4 stage and impairs the DN to DP transition

As the DN4 stage was likely to be perturbed by *Runx1* over-expression, we examined the degree of cell proliferation in *Runx1-tg* thymuses. Eight-week-old mice were injected intraperitoneally with BrdU, and their thymuses were harvested after 4 hr. Thymocytes were processed for four-colour flow cytometric analysis of BrdU, CD4/8, CD25 and CD44 (Fig. 6a). For the DN2 and DN3 fractions, the percentages of $BrdU^{+}$ cells were comparable between the *distal Runx1-tg;Lck-Cre-tg* (closed bars) and *Lck-Cre-tg* thymocytes (open bars). However, in the DN4 cells of the *distal Runx1-tg;Lck-Cre-tg* thymus, the per-

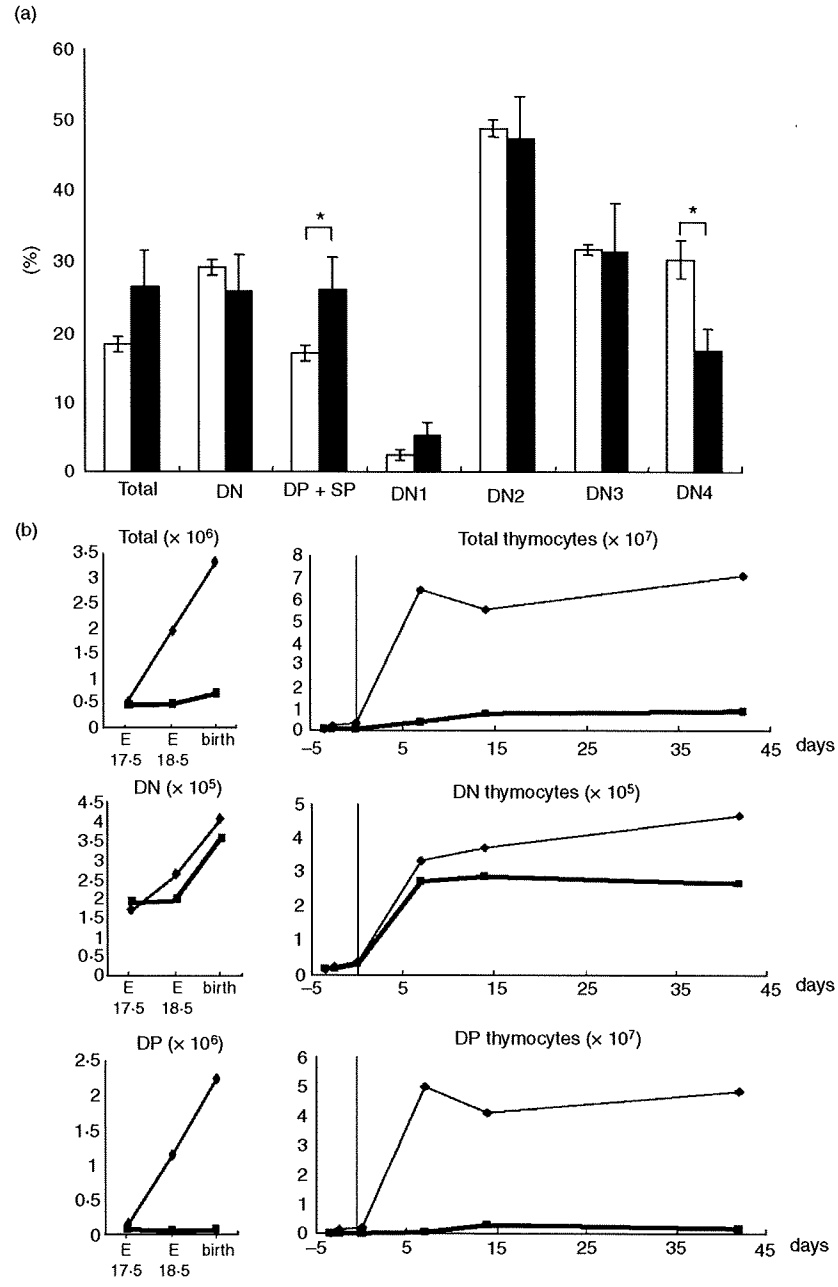

Figure 6. Effects of *Runx1-tg* on the growth and expansion of thymocytes. (a) Incorporation of bromodeoxyuridine (BrdU) into various subsets of thymocytes. *Lck-Cre-tg* mice (open boxes) and *distal Runx1-tg;Lck-Cre-tg* mice (closed boxes) were each injected with BrdU intraperitoneally. Thymocytes were prepared after 4 hr and processed for flow cytometric analysis of BrdU, CD4/CD8, CD25 and CD44. Percentages of $BrdU^+$ cells in various subsets are shown as the mean ± SD values ($n = 3$). Significances of difference were statistically tested by Student's *t*-test, and if detected between the compared genotypes, they are indicated by brackets with *($P < 0{\cdot}05$). (b) Ontogeny of DN and DP thymocytes during mouse development. Thymuses were taken from mice at embryonic day 17·5 (E17.5), E18.5, at birth, 1, 2 and 6 weeks after birth, and processed for flow cytometric analysis of CD4 and CD8 expression. The numbers of total, DN and DP cells are shown in *distal Runx1-tg;Lck-Cre-tg* (thick lines) and *Lck-Cre-tg* mice (thin lines).

centage of $BrdU^+$ cells was reduced to nearly half that of the control. An increase of the $BrdU^+$ percentage in the DP + SP fraction might reflect a compensatory growth enhancement in the *distal Runx1-tg;Lck-Cre-tg* thymuses. An essentially similar result was obtained when 1-week-old mice were used for the same experiments (data not shown). We conclude therefore that over-expression of *distal Runx1* impairs the ability of DN4 thymocytes to proliferate. It must be noted that the extent of apoptosis, as measured by Annexin V staining, was not enhanced in the *distal Runx1-tg;Lck-Cre-tg* thymocytes compared with the *Lck-Cre-tg* thymocytes (Fig. S3b).

Finally, we analysed thymocyte differentiation during mouse development. Thymuses were harvested at embryonic day (E) 17·5, E18·5, at birth and 1, 2 and 7 weeks after birth, from *distal Runx1-tg;Lck-Cre-tg* and *Lck-Cre-tg* mice, and processed for flow cytometric analysis with CD4, CD8 and Thy-1.2. The numbers of $Thy\text{-}1.2^+$ DN and DP cells were plotted together with the development and growth of the mice (Fig. 6b). There were slightly fewer DN cells in the *distal Runx1-tg;Lck-Cre-tg* thymuses (thick line) than in the *Lck-Cre-tg* thymuses (thin line) throughout the developmental stages examined. In contrast, the number of DP cells from the *distal Runx1-tg;Lck-Cre-tg* thymuses was remarkably diminished when compared with the *Lck-Cre-tg* cells. This difference was particularly marked 1 week after birth. This was because, during this period, the total cell number (consisting mainly of DP cells) increased

dramatically in the control thymus but not in the *Runx1-tg;Lck-Cre-tg* thymus. Taken collectively, the results illustrated in Fig. 6 indicated that over-expression of *distal Runx1* appears to severely disrupt the transition of thymocytes from the DN4 to DP stages.

Discussion

Previous studies have demonstrated that the abolition of *Runx1* expression causes severe impairments in the differentiation of DN thymocytes, highlighting an indispensable role for *Runx1* at this particular stage of T-cell development.[3,4,9] These targeting studies evaluated the significance of *Runx1* expression in DN cells; however, the Runx1 protein is then down-regulated during the transition from the DN to the DP stage. In this study, we investigated whether the down-regulation of Runx1, that accompanies the DN to DP differentiation, has biological significance. This was assessed using conditional *Runx1*-transgenic mice to disrupt the down-regulation of Runx1. *Lck-Cre*-mediated deletion has been shown to be initiated at DN2 and completed by DN3.[23] Therefore, the onset of *Runx1* transgene expression can be manipulated to start at the DN2 stage by mating *Runx1-tg* mice with *Lck* promoter-driven *Cre*-transgenic mice. When *Runx1* over-expression was initiated at such an early DN stage, it resulted in a marked impairment in the transition of cells from the DN to DP stages.

The DN-cell population is not a homogeneous entity, but rather comprises a population of developing cells with different characteristics divided into four subgroups (DN1 to DN4). For example, DN1 cells retain the potential to differentiate into B-cell and myeloid lineages, but they lose/reduce this capability once they have entered the DN2 stage.[24–29] The cells at a DN3 stage undergo a critical β-selection checkpoint. In the *distal Runx1-tg;Lck-Cre-tg* DN3 thymocytes, rearrangement of the *TCRβ* locus and pre-TCR expression did not appear to be affected.

On the other hand, in the same *distal Runx1-tg;Lck-Cre-tg* thymuses, the number of DN4 cells was substantially decreased, and the proportion of $CD27^{hi}$ (DN4) population was remarkably reduced. In parallel, an extent of cell growth, as measured by BrdU incorporation, was decreased by nearly half in these double-transgenic DN4 cells. Hence, the differentiation of *distal Runx1-tg;Lck-Cre-tg* thymocytes was probably perturbed during the DN4 stage and/or the DN4 to DP transition. The DN to DP transition is the step when cells rapidly undergo massive expansion as seen in the thymocyte ontogeny. Disruption in the normal processing of this transition is a likely explanation for the paucity of DP cells in *distal Runx1-tg;Lck-Cre-tg* thymuses (for example, if the normal growth rate decreased by half during each of four cell divisions, the resulting cell number would be one-sixteenth that of the *Lck-Cre-tg* control thymus).

In this study we have shown that the over-expression of *distal Runx1* is deleterious for the DN4 thymocytes. In contrast, *vav*-promoter driven, over-expression of *distal Runx1* is reported to be oncogenic in the T-cell lineage and to cause lymphoma in mice.[30,31] A clue for the apparently discrepant effects of Runx1 over-expression on thymocytes might be found in a study of *CD2-Runx2-tg* thymuses by Vaillant *et al.*[32] There, as in the present study, Runx2 over-expression causes anti-proliferative effects and a differentiation block at the DN to DP intermediate stage, but, unlike the present case, simultaneously and eventually brings about predisposition to lymphoma development. On the other hand, we previously reported that cell division in *TCR* and *Runt* (a dominant interfering form of *Runx1*) double-transgenic thymocytes was also moderately impaired during the DN4 to DP transition.[33] Considering together the previous reports and the present results, for the cells to pass safely through the critical DN4 point, a dosage of Runx1 must be adequately regulated within a rather narrow window.

The transcription of the *Runx1* gene is initiated either from the distal or proximal promoters.[10,11] This feature is conserved in all vertebrate *Runx* genes examined, and it is shared by all three members of the *Runx* gene family (Runx1, Runx2 and Runx3). The distal and proximal Runx1 proteins are identical to each other, except for the extreme N-terminal 19 (distal) and five (proximal) amino acid residues. Hence, the abolition of DP thymocytes by the over-expression of *distal Runx1*, but not *proximal Runx1*, can be ascribed solely to the differences in the N-termini of the two Runx1 isoforms. In fact, the distal Runx1 protein binds to a Runx consensus binding site with a two-fold to three-fold higher affinity than does the proximal Runx1 protein.[12] In addition, the distal and proximal forms of the Runx3 protein exhibit different activities in assays using Runx site-dependent reporter plasmids, in which only the N-terminal region of the distal, but not the proximal, Runx3 protein possesses transactivation capability.[34] Furthermore, the selective loss or transgenic over-expression of the proximal or distal Runx2 isoforms have been shown to cause differential effects on bone development in mice.[35,36] It is conceivable that the 19 amino acids of distal Runx1 (highly conserved with Runx2/3) also possess a unique transcriptional modulating activity, which influences DN-cell differentiation. It must be noted that the major species of Runx1 expressed and/or down-regulated in the thymus is a distal Runx1. This observation is in concordance with our observation that over-expression of distal, but not proximal, *Runx1* catastrophically impaired DN-cell development.

Acknowledgements

We would like to express our thanks to E.V. Rothenberg for helpful discussions. We also thank J. Takeda for

